RIKEN June, 2010

(expecting experimentalists for audience)

A revised version of the lecture slides given in Sept., 2007.

One-particle motion in nuclear many-body problem (V.1)

- from spherical to deformed nuclei - from stable to drip-line
- from static to rotating field - from particle to quasiparticle
- collective modes and many-body correlations in terms of one-particle motion

Ikuko Hamamoto

Division of Mathematical Physics, LTH,
University of Lund, Sweden

The figures with figure-numbers but without reference, are taken from

the basic reference : A.Bohr and B.R.Mottelson, Nuclear Structure, Vol. I & II

1. Introduction

Mean-field approximation to many-body system

The study of one-particle motion in the mean field is the basis for understanding not only single-particle mode but also many-body correlation.

Mean field ⟵ Hartree-Fock approximation

Self-consistent potential = Hatree-Fock potential

Phenomenological one-body potential

(convenient for understanding the physics in a simple terminology and in a systematic way)

Harmonic-oscillator potential

Woods-Saxon potential

Note, for example,

the shape of a many-body system can be obtained only from the one-body density

⟵ mean-field approximation

Harmonic-oscillator potential is exclusively used, for example,
the system with a finite number of electrons bound by an external field
(= a kind of NANO structure system).
This system is a sufficiently bound system so that harmonic-oscillator potential is a good approximation to the effective potential.

Another finite system to which quantum mechanics is applied is
clusters of metalic atoms

$\longrightarrow$ shell-structure based on one-particle motion of electrons.

In this system a harmonic-oscillator potential is also often used.

2. Mean-field approximation to spherical nuclei

2.1. Phenomenological one-body potentials

3-dimensional harmonic oscillator potential

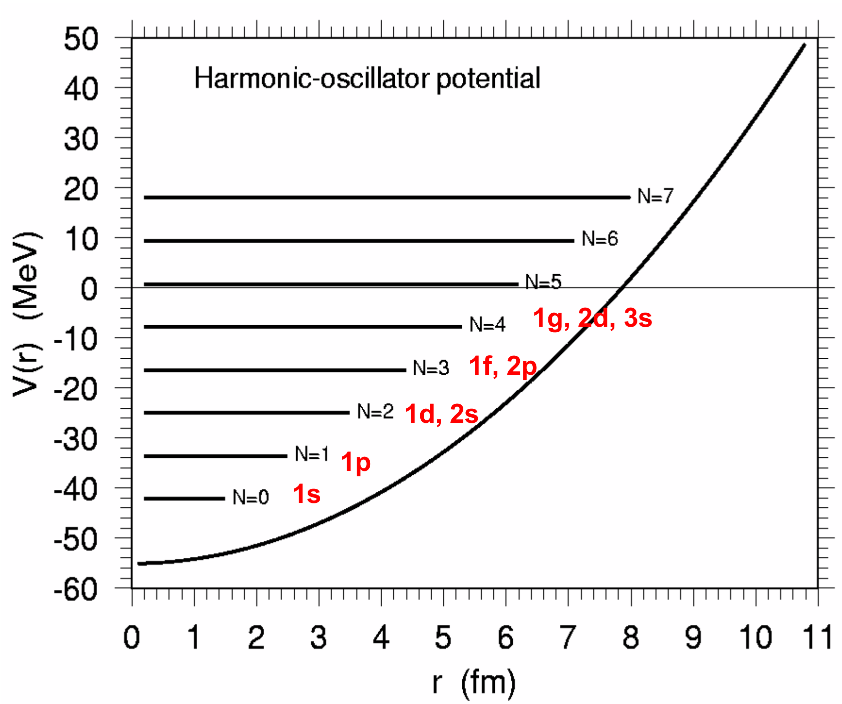

In the above figure

$$V(r) = \frac{1}{2} m\omega^2 r^2 + \underline{const}$$

where const = –55 MeV

$\hbar\omega$ = 8.6 MeV

$$H = -\frac{\hbar^2}{2m}\Delta + \underline{\frac{1}{2} m\omega^2 r^2}$$

harmonic-oscillator potential

has a spectrum

$$\varepsilon = \left(N + \frac{3}{2}\right)\hbar\omega$$

where

$$N = n_x + n_y + n_z \qquad \text{in rectilinear coordinates}$$

$$= 2(n_r - 1) + \ell \qquad \text{in polar coordinates}$$

ℓ = *N, N-2, … 0 or 1*

Degeneracy of the major shell with a given *N*

$$\sum_\ell 2(2\ell + 1) = (N+1)(N+2)$$

spin ↑↓ (ℓ = even for N=even, odd for N=odd)

leads to the magic numbers

2, 8, 20, 40, 70, 112, 168, …

One-particle levels for β stable nuclei

($S_n \approx S_p \approx$ 7-10 MeV)

Modified harmonic-oscillator potential can often be a good approximation.

Large energy gap in one-particle spectra

↔ Magic number
N, Z = 8, 20,28,50,82,126, …

Nuclei with magic number : spherical shape

Normal-parity orbits ← majority in a major shell of medium-heavy nuclei

High-j orbits, $1g_{9/2}$, $1h_{11/2}$, $1i_{13/2}$, $1j_{15/2}$,
which have parity different from the neighboring orbits do not mix with them under quadrupole ($Y_{2\mu}$) deformation and rotation.

One-particle motion in the mean-field
→ shell structure (= bunching of one-particle levels)
→ nuclear shape

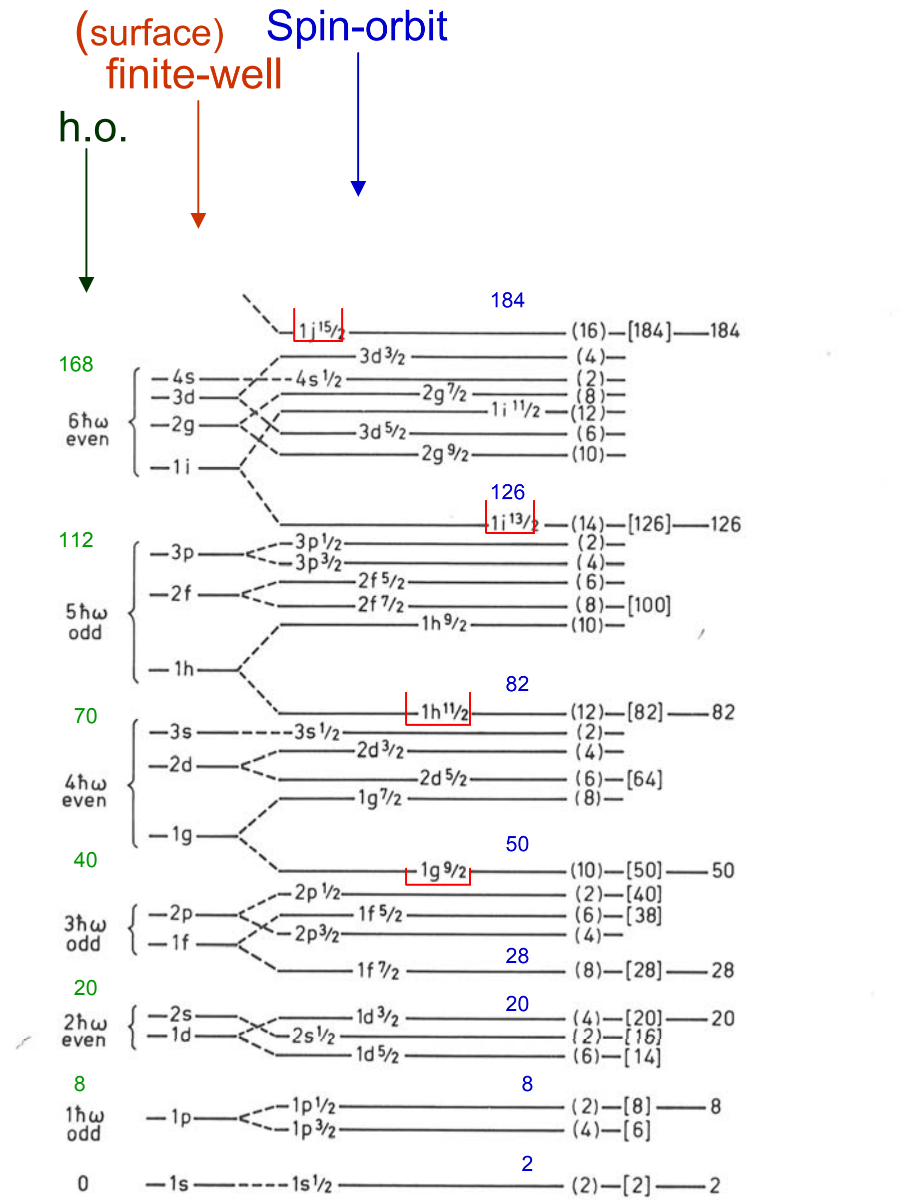

Figure 2-23 Sequence of one-particle orbits. The figure is taken from M. G. Mayer and

Phenomenological finite-well potential :

Woods-Saxon potential - an approximation to Hartree-Fock (HF) potential

$$V(r) = V_{WS}\, f(r) \qquad \text{where} \qquad f(r) = \frac{1}{1+\exp\left(\frac{r-R}{a}\right)}$$

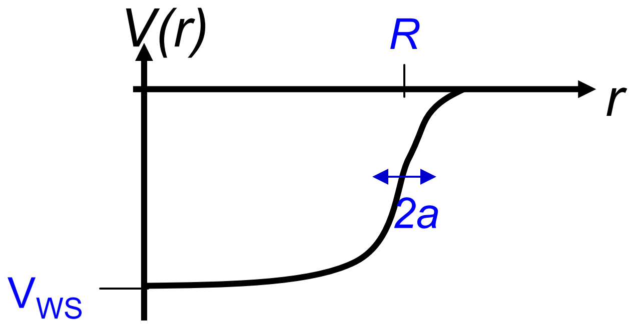

a : diffuseness

R : radius $\qquad R = r_0\, A^{1/3}$

A : mass number

standard values of parameters

$r_0 \approx 1.27$ fm $\qquad$ a $\approx$ 0.67 fm

$$V_{WS} = \left(-51 \pm 33\frac{N-Z}{A}\right) \text{ MeV}$$ for
+ for neutrons
– for protons

Woods-Saxon potential vs. harmonic-oscillator potential

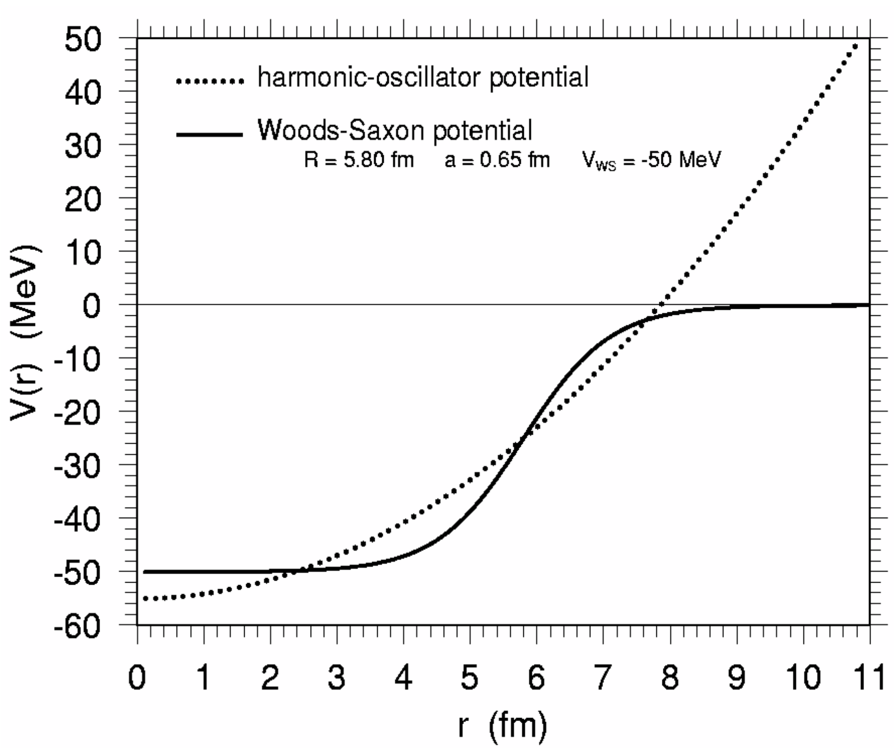

higher ℓ one-particle wave-functions

only ℓ=0 one-particle wave-funcions

In the above figure the parameters are chosen so that the root-mean-square radius for the two potentials, are approximately equal.

Harmonic-oscillator potential cannot be used for weakly-bound or unbound (or resonant) levels.

For well-bound levels;

Corrections to harmonic-oscillator potential are;

a) repulsive effect for short and large distances

→ push up small ℓ orbits

b) attractive effect for intermediate distances

→ push down large ℓ orbits

Schrödinger equation for one-particle motion with spherical finite potentials

$$H = -\frac{\hbar^2}{2m}\left(\frac{\partial^2}{\partial x^2} + \frac{\partial^2}{\partial y^2} + \frac{\partial^2}{\partial z^2}\right) + V(r) + V_{\ell s}(r)$$

(x, y, z) $\longrightarrow$ *(r, θ, φ)*

$$H\Psi = \varepsilon\Psi \qquad \Psi = \frac{1}{r}R_{n\ell j}(r)X_{\ell j m_j}(\hat{r})$$

where

$$X_{\ell j m_j}(\hat{r}) = \sum_{m_\ell, m_s} C(\ell, \frac{1}{2}, j; m_\ell, m_s, m_j) Y_{\ell m_\ell}(\theta, \phi)\chi_{1/2, m_s}$$

$$(\vec{\ell})^2 Y_{\ell m}(\theta,\phi) = \hbar^2 \ell(\ell+1) Y_{\ell m}(\theta,\phi)$$

The Shrödinger equation for radial wave-functions is written as

$$\left\{\frac{d^2}{dr^2} - \frac{\ell(\ell+1)}{r^2} + \frac{2m}{\hbar^2}\left(\varepsilon_{n\ell j} - V(r) - V_{\ell s}(r)\right)\right\} R_{n\ell j}(r) = 0 \qquad (\$)$$

For example, for neutrons eq.($) should be solved with the boundary conditions;

k_ℓ : Modified spherical Bessel function of the third kind (See p.443 of Abramowitz & Stegun, Handbook of mathematical functions)

j_ℓ : spherical Bessel function
n_ℓ : spherical Neumann function

at *r* = 0 $\qquad R_\ell(r) = 0$

at *r* → large (where *V(r)* = 0)

for $\varepsilon_\ell < 0$ $\qquad R_\ell(r) \propto \alpha r k_\ell(\alpha r)$ $\qquad$ where $\alpha^2 = -\frac{2m}{\hbar^2}\varepsilon_\ell$

for $\varepsilon_\ell > 0$ $\qquad R_\ell(r) \propto \cos(\delta_\ell) kr j_\ell(kr) - \sin(\delta_\ell) kr n_\ell(kr)$ $\qquad$ where $k^2 = \frac{2m}{\hbar^2}\varepsilon_\ell$

δ_ℓ : phase shift

One-body spin-orbit potential in phenomenological potentials : surface effect !

In the central part of nuclei the density, *ρ(r)* = const.
Then, the only direction, which nucleons can feel is the momentum, $\vec{p}$

From the two vectors, $\vec{p}$ and the spin $\vec{s}$, of nucleons one cannot make

P-inv (i.e. reflection-invariant) and *T*-inv (i.e. time-reversal invariant)

quantity linear in the momentum. For example,

$(\vec{p}\cdot\vec{s})$ ~~*P*-inv~~

$(\vec{p}\times\vec{s})\cdot\vec{s}$ ~~*T*-inv~~

At the nuclear surface $\vec{\nabla}\rho(r)\neq 0$ i.e. $\vec{\nabla}\rho(r)=\left(\frac{\partial\rho}{\partial r},0,0\right)$ in polar coordinate (r,θ,φ)

$$\vec{r}=(r,0,0)$$

$$\vec{r}\times\vec{p}=(0,-rp_\phi,rp_\theta)$$

Then, $(\vec{p}\times\vec{s})\cdot\vec{\nabla}\rho(r)$: *P*-inv & *T*-inv !

$$=(p_\theta s_\phi-p_\phi s_\theta)\frac{\partial\rho}{\partial r}\quad=\frac{1}{r}\left((\vec{r}\times\vec{p})\cdot\vec{s}\right)\frac{\partial\rho}{\partial r}$$

$$=(\vec{\ell}\cdot\vec{s})\frac{1}{r}\frac{\partial\rho}{\partial r}$$

In practice, one often uses the form

$$V_{\ell s}(r)=\lambda(\vec{\ell}\cdot\vec{s})\frac{1}{r}\frac{\partial V_c(r)}{\partial r}$$

where λ=const. and $V_c(r)$ is one-body central potential such as the Woods-Saxon potential

In the presence of spin-orbit potential $V_{\ell s}(r)$ ($\propto (\vec{\ell}\cdot\vec{s})$) ,
the total angular momentum of nucleons

$$\vec{j} = \vec{\ell} + \vec{s} \qquad j = \ell \pm \frac{1}{2}$$

becomes a good quantum-number.

$$\left[(\vec{\ell}\cdot\vec{s}), \ell_z\right] \neq 0$$

$$\left[(\vec{\ell}\cdot\vec{s}), s_z\right] \neq 0$$

$$\left[(\vec{\ell}\cdot\vec{s}), \ell_z + s_z\right] = 0$$

$$H = -\frac{\hbar^2}{2m}\Delta + V(r)$$ → quantum number of one-particle motion (ℓ , s , m_ℓ , m_s)

$$H = -\frac{\hbar^2}{2m}\Delta + V(r) + V_{\ell s}(r)$$ → quantum number of one-particle motion (ℓ , s , j , m_j)

$$(\vec{\ell}\cdot\vec{s}) = \frac{1}{2}\left\{\vec{j}^2 - \vec{\ell}^2 - \vec{s}^2\right\} = \frac{1}{2}\left\{j(j+1) - \ell(\ell+1) - \frac{1}{2}(\frac{1}{2}+1)\right\} = \begin{cases} -\ell-1 & \text{for } j = \ell - 1/2 \\ \ell & \text{for } j = \ell + 1/2 \end{cases}$$

$$H\Psi = \varepsilon\Psi$$

$$\Psi = \frac{1}{r}R_{\ell j}(r)X_{\ell j m_j}$$ where $$X_{\ell j m_j} \equiv \sum_{m_\ell, m_s} C(\ell, \frac{1}{2}, j; m_\ell, m_s, m_j) Y_{\ell m_\ell}(\theta,\phi)\chi_{1/2, m_s}$$

The radial part of the Schrödinger equation becomes

$$\left\{\frac{d^2}{dr^2} - \frac{\ell(\ell+1)}{r^2} + \frac{2m}{\hbar^2}\left(\varepsilon_{\ell j} - V(r) - V_{\ell s}(r)\right)\right\} R_{\ell j}(r) = 0$$

Centrifugal potential + Woods-Saxon potential —— dependence on ℓ

$$-\frac{\hbar^2}{2m}\left(\frac{\partial^2}{\partial x^2}+\frac{\partial^2}{\partial y^2}+\frac{\partial^2}{\partial z^2}\right)+V(r)$$

$$=-\frac{\hbar^2}{2m}\left(\frac{1}{r}\frac{\partial^2}{\partial r^2}r+\frac{1}{r^2}\left(\frac{\partial^2}{\partial\theta^2}+\cot\theta\frac{\partial}{\partial\theta}+\frac{1}{\sin^2\theta}\frac{\partial^2}{\partial\phi^2}\right)\right)+V(r)$$

$$=\ -\frac{\hbar^2}{2m}\left(\frac{1}{r}\frac{\partial^2}{\partial r^2}r-\underbrace{\frac{1}{r^2}\frac{(\vec{\ell})^2}{\hbar^2}}_{\text{centrifugal potential}}\right)+V(r)$$

$\ell = 0$

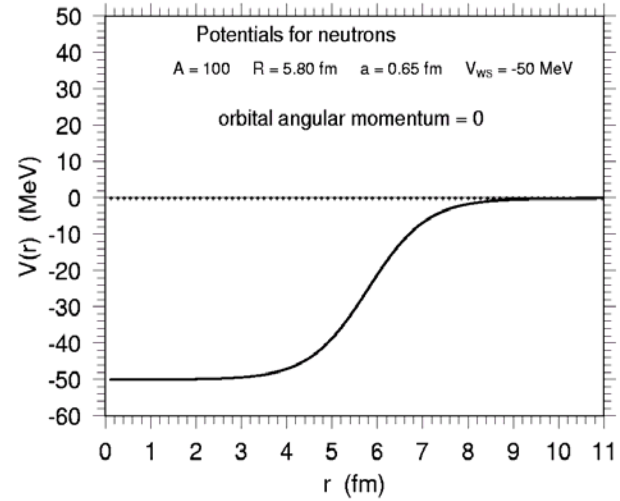

$\ell = 2$

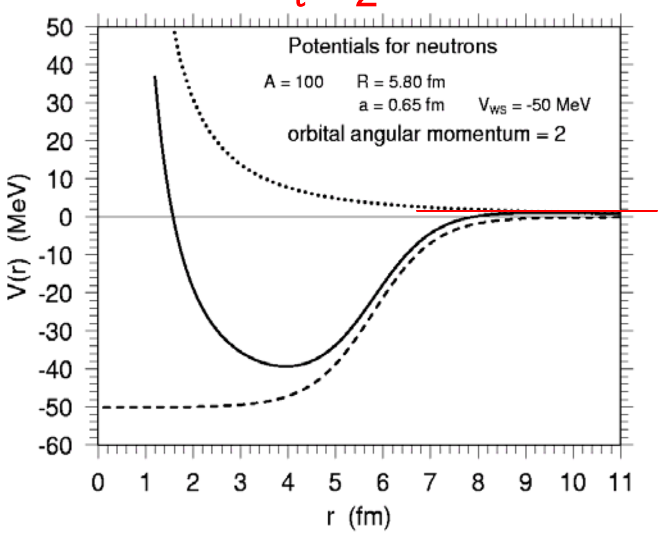

$\ell = 4$

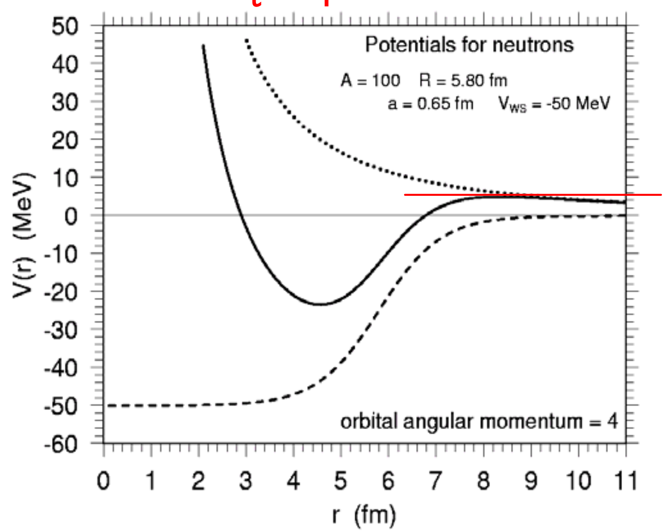

- - - - Woods-Saxon pot.

.... centrifugal pot.

——— W-S + centrifugal pot.

Height of centrifugal barrier $\propto \dfrac{\ell(\ell+1)}{R_h^{\;2}}$ where $R_h > r_0 A^{1/3}$

The height : $\begin{cases} \text{higher for smaller nuclei} \\ \text{higher for larger } \ell \text{ orbits} \end{cases}$

ex. For the Woods-Saxon potential with R=5.80 fm, a=0.65 fm, r_0 =1.25 and V_{WS} = – 50 MeV ;

ℓ	height of centrifugal barrier
0	0 MeV
1	≈ 0.4
2	≈ 1.3
3	≈ 2.8
4	≈ 5.1
5	≈ 8.2

Height of centrifugal barrier ;

1) well-bound particles are insensitive.

2) affects eigenenergies and wave-functions of weakly-bound neutrons, especially with small ℓ

3) affects the presence (or absence) of one-particle resonance, resonant energies and widths.

Neutron radial wave-functions

$$\Psi_{n\ell jm}(\vec{r}) = \frac{1}{r}\underline{R_{n\ell j}(r)}X_{\ell jm}(\hat{r})$$

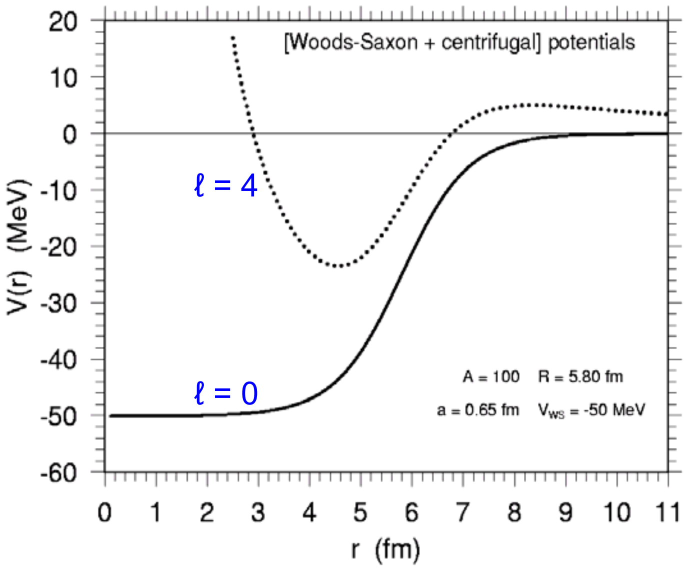

ε = – 8 MeV

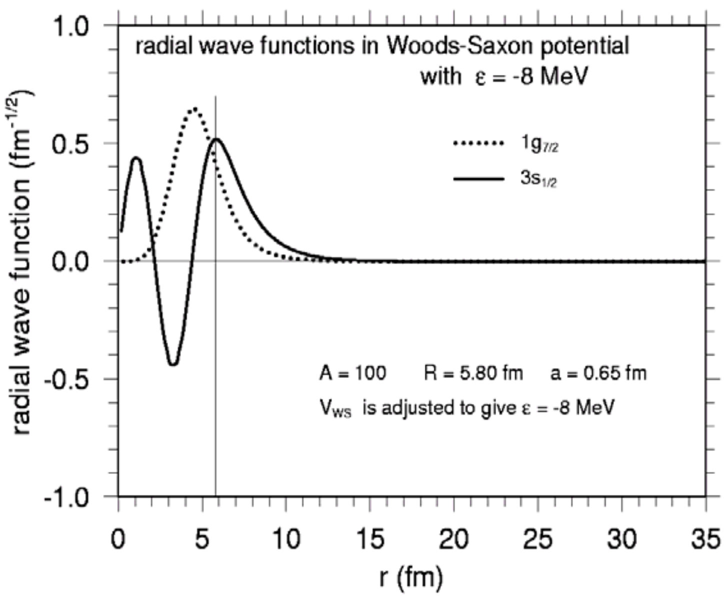

ε = – 200 keV

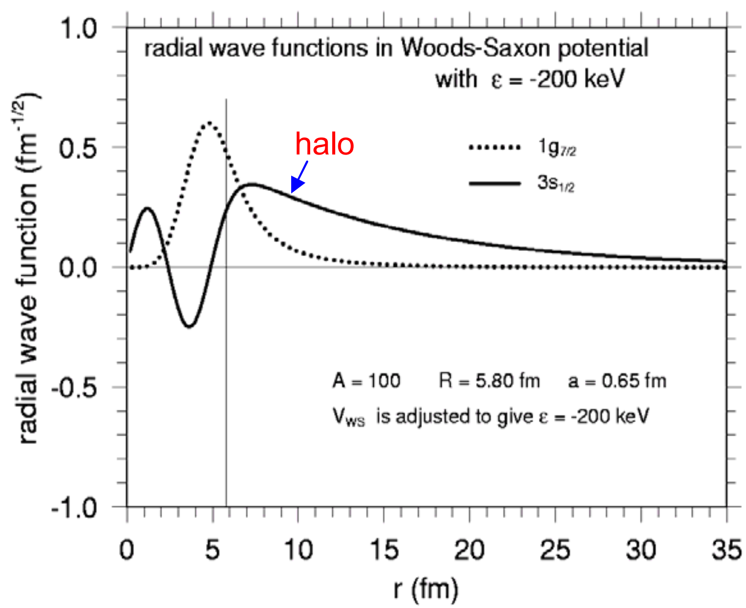

For a finite square-well potential

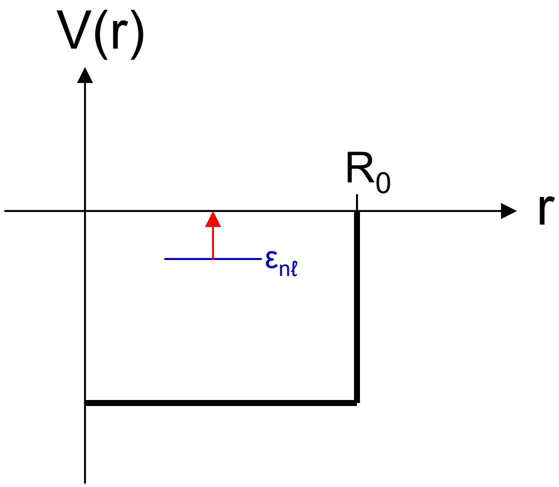

The probability for one neutron to stay inside the potential, when the eigenvalue $\varepsilon_{n\ell}$ $(< 0) \rightarrow 0$

ℓ	0	1	2	3	ℓ ($\neq$0)
$\int_0^{R_0} \lvert R_{n\ell}(r) \rvert^2 \, dr$	0	1/3	3/5	5/7	$(2\ell-1)/(2\ell+1)$

Root-mean-square radius, r_{rms}, of one neutron ; $r_{rms} \equiv \sqrt{\langle r^2 \rangle}$

In the limit of $\varepsilon_{n\ell}$ $(<0) \rightarrow 0$

$$r_{rms} \propto (-\varepsilon_{n\ell})^{-1/2} \longrightarrow \infty \qquad \text{for } \ell = 0$$

$$(-\varepsilon_{n\ell})^{-1/4} \longrightarrow \infty \qquad \text{for } \ell = 1$$

finite value for $\ell \geq 2$

Spherical nuclei : unique behavior of low-ℓ orbits, as $\varepsilon_\ell(<0) \rightarrow 0$

Energies of neutron orbits in Woods-Saxon potential
($R = r_0 A^{1/3}$ with $r_0 = 1.27\ fm$ is varied.)

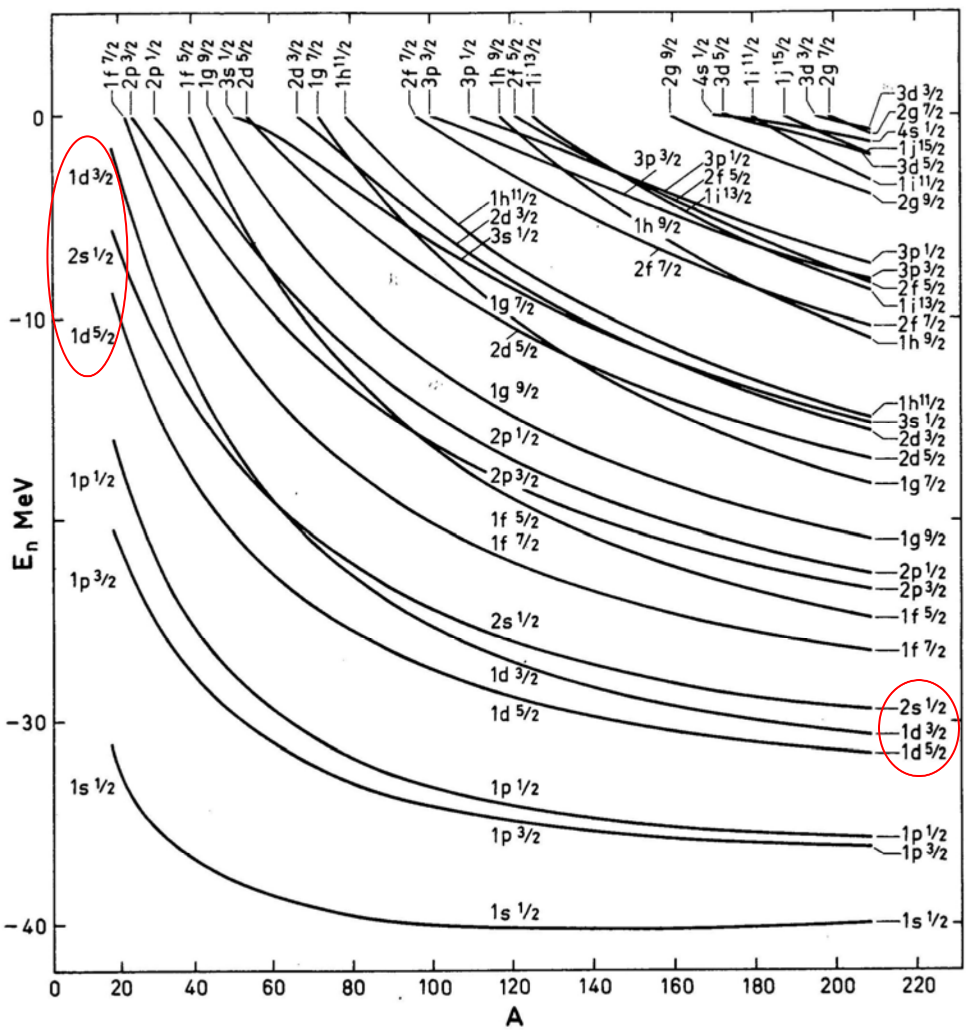

Figure 2-30 Energies of neutron orbits calculated by C. J. Veje (private communication).

Change of shell structure

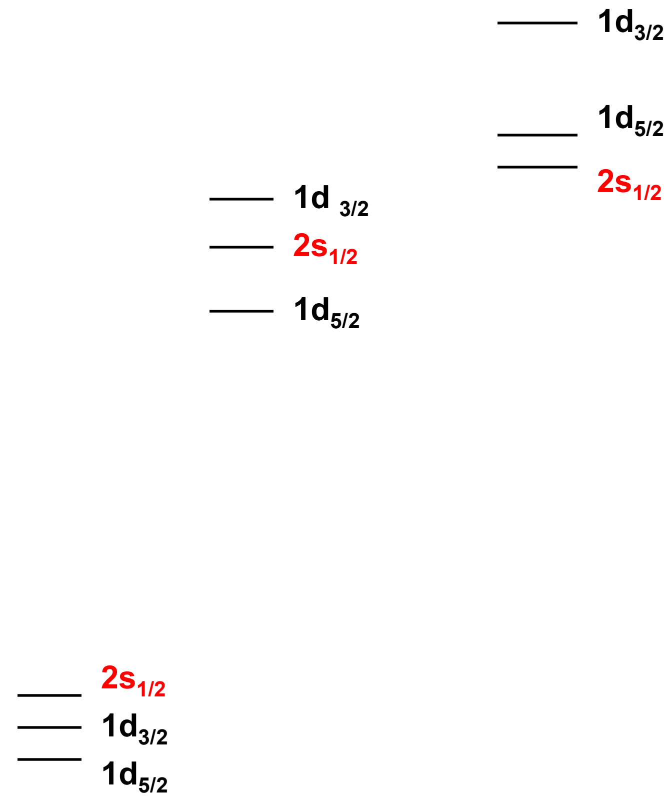

Strongly bound | **Stable *sd*-shell nuclei** | **Very weakly bound**

in finite-well potential

There is no neutron ℓ=0 (s) resonance !

One-particle resonant level in spherical finite potentials (~~Coulomb potential~~)

For $\varepsilon_\ell > 0$ and $r \longrightarrow$ large

$$R_\ell(r) \propto \cos(\delta_\ell) krj_\ell(kr) - \sin(\delta_\ell) krn_\ell(kr) \qquad \text{where} \qquad k^2 \equiv \frac{2m}{\hbar^2}\varepsilon_\ell$$

δ_ℓ : phase shift

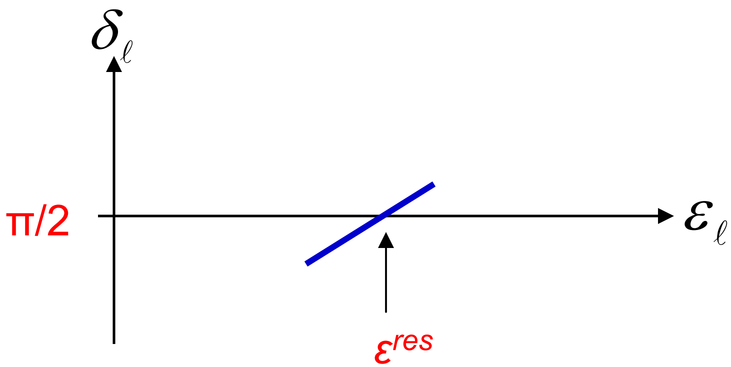

The width of the resonance;

$$\Gamma \equiv \frac{2}{\left.\dfrac{d\delta}{d\varepsilon}\right|_{\varepsilon=\varepsilon^{res}}}$$

The resonance energy ε^{res} is defined so that the phase shift δ_ℓ increases with energy ε as it goes through π/2 (modulo π).

For example, see ; R.G.Newton, *SCATTERING THEORY OF WAVES AND PARTICLES,* McGraw-Hill, 1966.

At ε^{res} ; (1) a sharp peak in the scattering cross section;
(2) a significant time delay in the emergence of scattered particles;
(3) the incoming wave (i.e. particles) can strongly penetrate into the system;
(4) ………..

Resonance $\leftrightarrow$ time delay $\leftrightarrow$ $\left.\frac{d\delta_\ell}{dk}\right|_{k=k_0} > 0$

scattering amplitude $\quad f(k,\cos\theta) = k^{-1}\sum_{\ell=0}^{\infty}(2\ell+1)e^{i\delta_\ell}\sin\delta_\ell P_\ell(\cos\theta)$

For $r \to \infty$, a wave packet in a scattering is written as

$$\int d\vec{k}\,\phi(\vec{k})\exp\left[i(\vec{k}\cdot\vec{r}-Et)\right]+\int d\vec{k}\,\phi(\vec{k})r^{-1}\exp\left[i(kr-Et)\right]f(k,\cos\theta) \qquad (\$)$$

where $\phi(\vec{k})$: sharply peaked around $\vec{k} = \vec{k}_0$

Assume that at $k=k_0$ a sharp peak only in a given ℓ channel.

For very large t (= time), the 2nd term in ($) contributes only at the distance

$$r \cong \frac{k_0}{2m}t - \left.\frac{d\delta_\ell}{dk}\right|_{k=k_0}$$

$\because$) for $k \approx k_0$ $\quad \delta_\ell(k) \approx \delta_\ell(k_0) + \left.\frac{d\delta_\ell}{dk}\right|_{k=k_0}(k-k_0)$

$$e^{i(kr-Et)}e^{ik\left.\frac{d\delta_\ell}{dk}\right|_{k=k_0}} = e^{ik\left(r+\left.\frac{d\delta_\ell}{dk}\right|_{k=k_0}-\frac{k}{2m}t\right)}$$

Time delay caused by the sharply changing term $e^{i\delta_\ell}$ in the f: $\quad t_D = \frac{2m}{k_0}\left.\frac{d\delta_\ell}{dk}\right|_{k=k_0}$

$\frac{d\delta_\ell}{dk} > 0 \quad \to$ time delay in the emergence of the scattered particles

$\frac{d\delta_\ell}{dk} < 0 \quad \to$ time advance !

β-stable nuclei

One-particle levels which contribute to many-body correlations

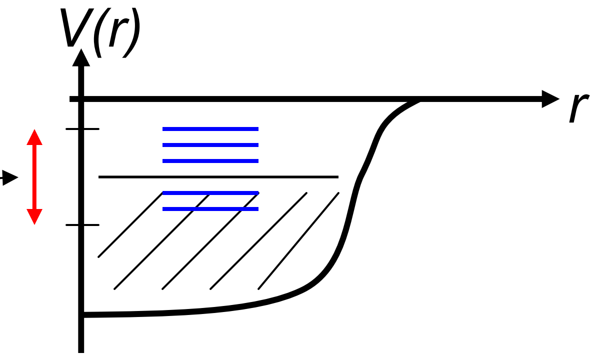

neutron drip line nuclei – role of continuum levels and weakly-bound levels

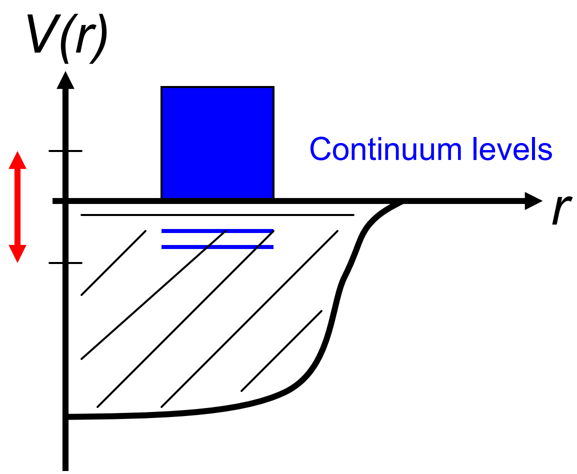

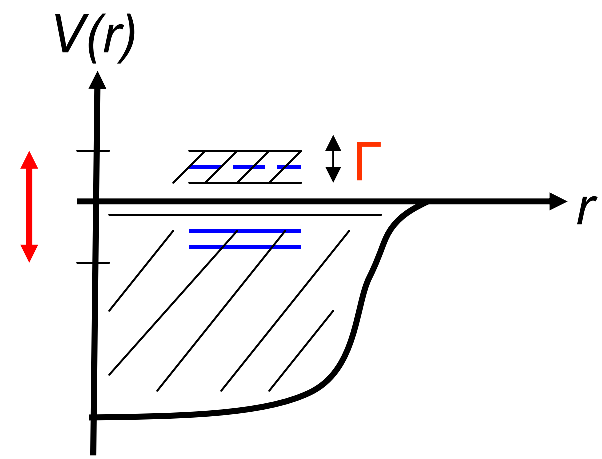

Importance of one-particle resonant levels with small width Γ in the many-body correlations.

Obs. no one-particle resonant levels for $\ell = 0$ (i.e. s) orbits.

Some summary of weakly-bound and positive-energy neutrons in spherical potentials ($\beta=0$)

Unique role played by neutrons in small ℓ ; s, p orbits

(a) Weakly-bound small-ℓ neutrons have appreciable probability to be outside the potential;

ex. For a finite square-well potential and $\varepsilon_{n\ell j}$ (<0) $\rightarrow 0$, the probability inside is

0 for s neutrons

1/3 for p neutrons

Thus, those neutrons are insensitive to the strength of the potential.

$\longrightarrow$ Change of shell-structure

(b) No one-particle resonant levels for s neutrons.

For a given $\varepsilon_{\ell j} > 0$, higher-ℓ orbits have one-particle resonance with smaller width.

One-particle neutron resonance with lower-ℓ disappears at a smaller $\varepsilon_{\ell j}$ (> 0) value.

$\longrightarrow$ Change of many-body correlation, such as pair correlation and deformation in nuclei with weakly-bound neutrons

2.2. Hartree-Fock (HF) approximation $\longrightarrow$ self-consistent mean-field

A mean-field approximation to the nuclear many-body problem with rotationally invariant Hamiltonian,

$$H = -\frac{\hbar^2}{2m}\sum_i \Delta_i + \underbrace{\sum_{i<j} v_{ij}}$$

"effective" two-body interaction

phenomenology !

Popular effective interaction, v_{ij} , is so-called Skyrme interaction – many different versions exist, but

in essence, $\delta(\vec{r}_i - \vec{r}_j)$ interaction

plus density-dependent part that simulates the 3-body interaction.

The total wave function Ψ is assumed to be a form of Slater determinant consisting of one-particle wave-functions,

$\varphi_i(\vec{r}_j)$ *(i and j) = 1, 2, ….., A*

Variational principle $\delta\left\langle \Psi \,|\, H \,|\, \Psi \right\rangle = 0$

together with subsidiary conditions $\int |\varphi_i(\vec{r}_i)|^2 \, d^3 r_i = 1$

leads to the HF equation.

OBS. The HF solution Ψ is not an eigen function of the Hamiltonian *H.*

ex. HF equations for 2 particles (a simple example !)

$$\Psi(1,2) = \frac{1}{\sqrt{2}} \begin{vmatrix} \varphi_1(\vec{r}_1) & \varphi_2(\vec{r}_1) \\ \varphi_1(\vec{r}_2) & \varphi_2(\vec{r}_2) \end{vmatrix}$$

$$\begin{cases} -\dfrac{\hbar^2}{2m}\Delta\varphi_1(\vec{r}_1) + \varphi_1(\vec{r}_1)\underline{\int \varphi_2^*(\vec{r})v(\vec{r}_1,\vec{r})\varphi_2(\vec{r})d^3r} - \underline{\varphi_2(\vec{r}_1)\int \varphi_2^*(\vec{r})v(\vec{r}_1,\vec{r})\varphi_1(\vec{r})d^3r} = \varepsilon_1\varphi_1(\vec{r}_1) \\ -\dfrac{\hbar^2}{2m}\Delta\varphi_2(\vec{r}_2) + \varphi_2(\vec{r}_2)\underline{\int \varphi_1^*(\vec{r})v(\vec{r}_2,\vec{r})\varphi_1(\vec{r})d^3r} - \underline{\varphi_1(\vec{r}_2)\int \varphi_1^*(\vec{r})v(\vec{r}_2,\vec{r})\varphi_2(\vec{r})d^3r} = \varepsilon_2\varphi_2(\vec{r}_2) \end{cases}$$

exchange (Fock) term (absent in Hartree approximation)

Hartree potential $V_H(\vec{r}_1)$ and $V_H(\vec{r}_2)$

Find the solutions, $\varphi_1(\vec{r})$ and $\varphi_2(\vec{r})$, with ε_1 and ε_2 , which satisfy simultaneously the above coupled equations.

The usual procedure of solving the HF equation is;

$$\boxed{\text{w.f.} \quad \begin{matrix}\varphi_1(\vec{r}_1) \\ \varphi_2(\vec{r}_2)\end{matrix}} \longrightarrow \boxed{\text{pot.} \quad \begin{matrix}V(\vec{r}_1) \\ V(\vec{r}_2)\end{matrix}} \longrightarrow \boxed{\text{w.f.} \quad \begin{matrix}\varphi_1(\vec{r}_1) \\ \varphi_2(\vec{r}_2)\end{matrix}} \longrightarrow$$

Find self-consistent solutions together with eigenvalues, ε_1 and ε_2 .

drip-line nuclei —— very different N/Z ratio, compared to stable nuclei with a given A

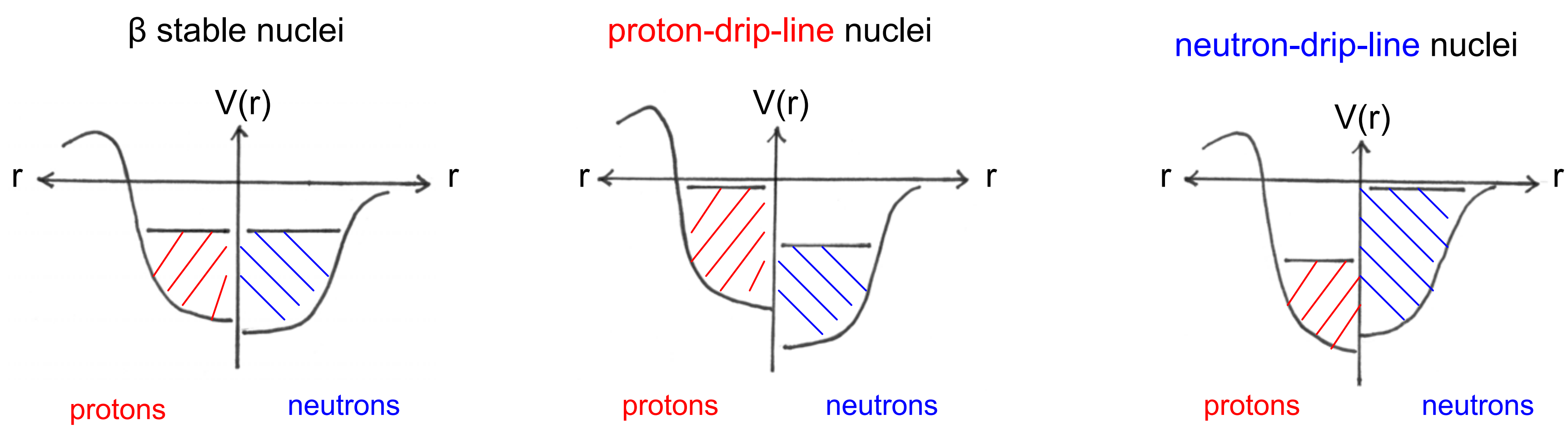

Since the Fermi levels for protons and neutrons are very different in drip line nuclei, this binding energy difference of least-bound protons and neutrons will produce interesting phenomena in charge-exchange reactions or β decays.

Weakly-bound one-proton motion in medium-heavy nuclei may not be so different from the well-bound one, due to the high Coulomb barrier.

Hartree-Fock potential and one-particle energy levels

$V_N(r)$: neutron potential, $V_P(r)$: proton nuclear potential, $V_P(r)+V_C(r)$: proton total potential

A typical double-magic β-stable nucleus

$$^{208}_{82}Pb_{126}$$

One of Skyrme interactions ;

SkM*

See : J.Bartel et al., Nucl. Phys. A386 (1982) 79.

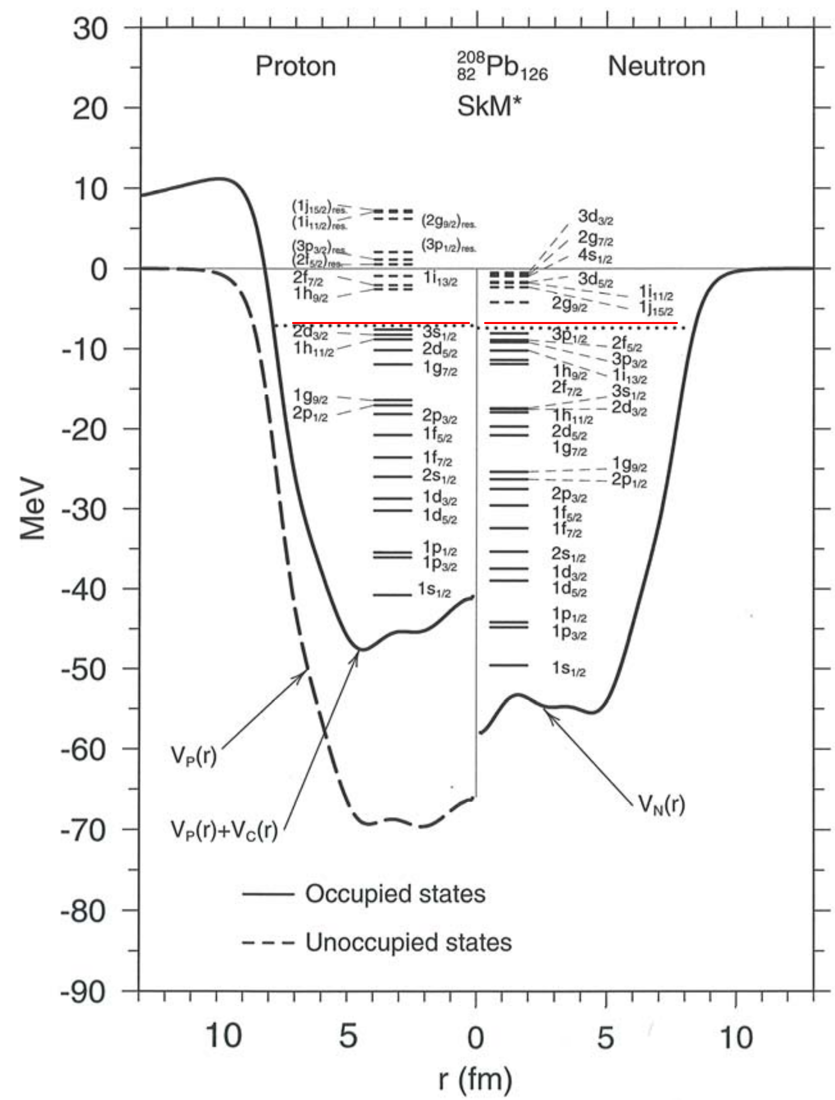

Hartree-Fock potentials and one-particle energy levels

$V_N(r)$: neutron potential, $V_P(r)$: proton nuclear potential

ex. of neutron-drip-line nuclei

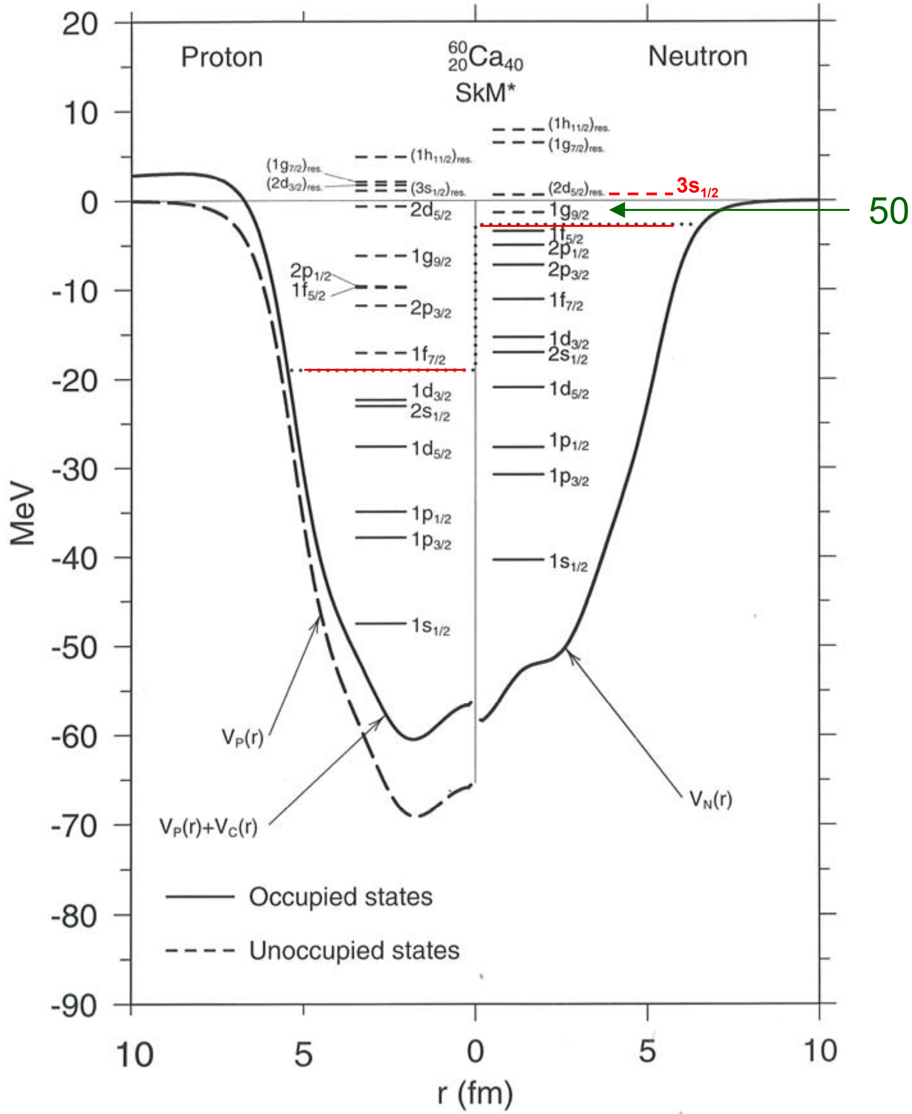

ex. of proton-drip-line nuclei

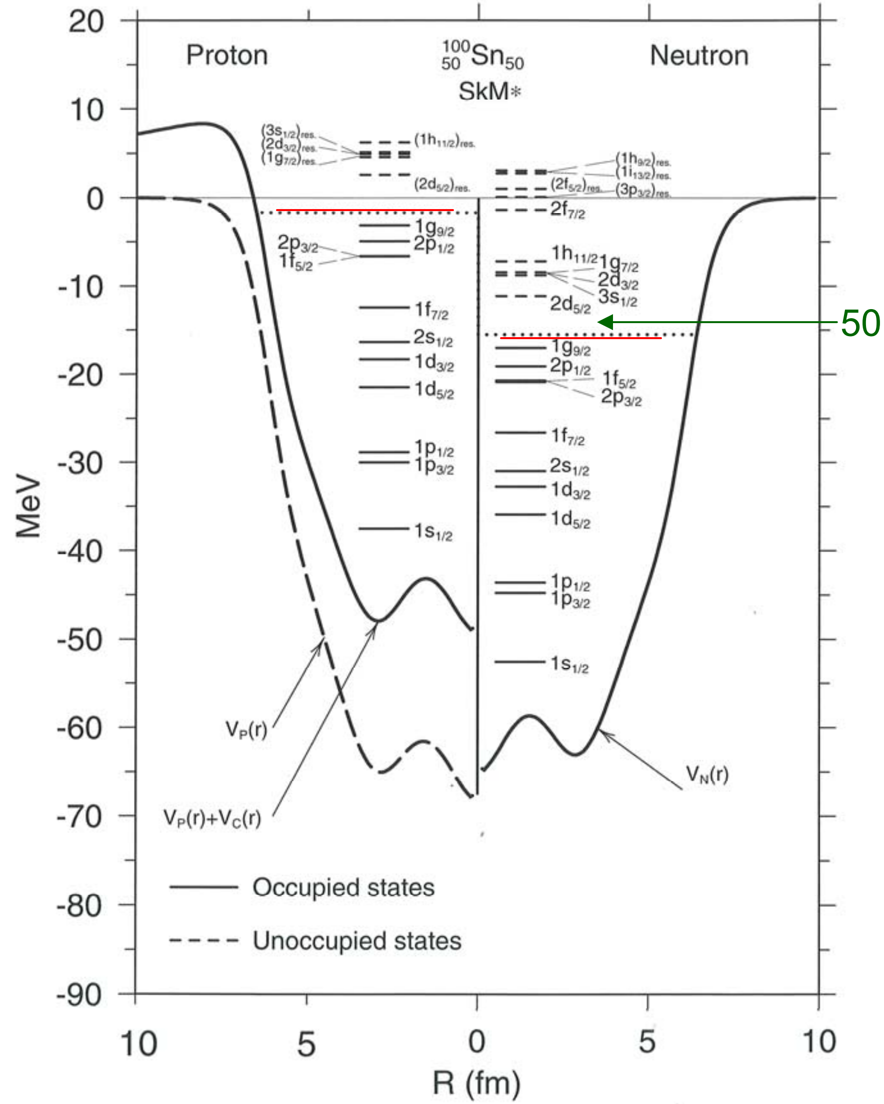

3. Observation of deformed nuclei

3.1. Rotational spectrum and its implication

Some nuclei are deformed --- axially-symmetric quadrupole (Y20) deformation

Observation :

1) rotational spectra $E(I) \approx AI(I+1)$

2) large quadrupole moment or large $E2(I \rightarrow I-2)$ transition probability

rotation of deformed nuclei → time-dependent electric field → strong el-mag radiation

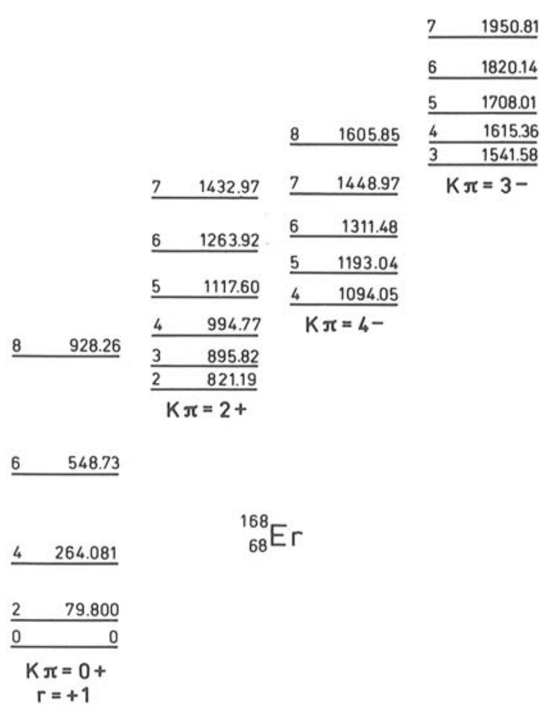

Figure 4-7 Spectrum of ^{168}Er. The data are taken from H. R. Koch, *Z. Physik* **192**, 142

For $E(I) = AI(I+1)$,

$$\frac{E(I=4)}{E(I=2)} = 3.33$$

ex. In the ground band of ^{168}Er

$$\frac{264.081}{79.800} = 3.31$$

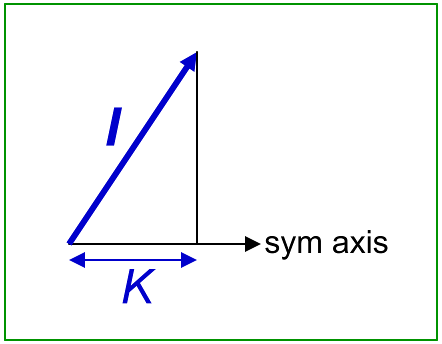

A rotational band with a given K consists of members with $I \geq K$.

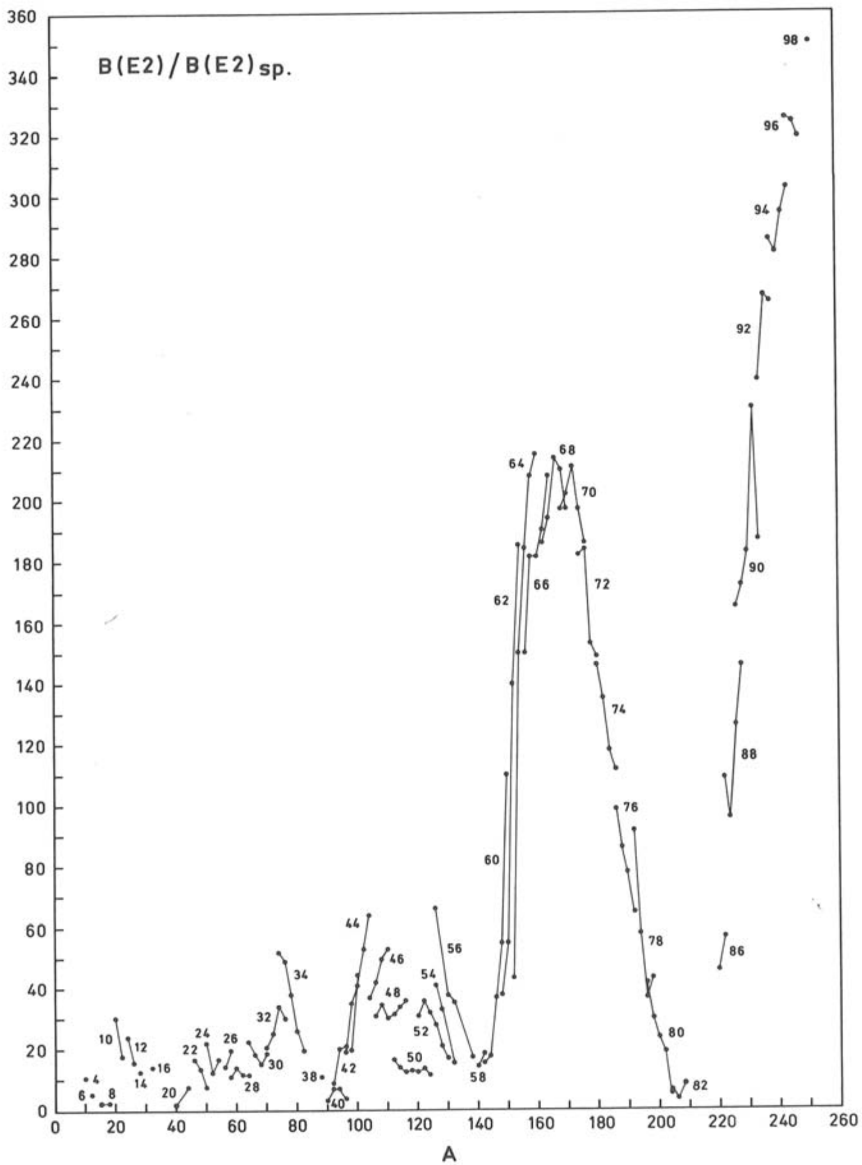

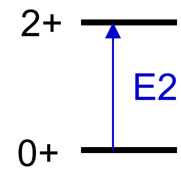

Observed E2-transition probabilities from the ground state ($I^{\pi}=0^{+}$) to the first excited 2^{+} state in stable even-even nuclei.

The single-particle value used as unit is

$$B_{sp}(E2) = \frac{5}{4\pi} e^2 \left(\frac{3}{5} R^2 \right)^2 = 0.30 A^{4/3} e^2 \, fm^4$$

Bohr & Mottelson, Nuclear Structure, Vol.II, 1975, Fig.4-5

WARNING : many different definitions (and notations) of Y_{20} deformation parameters

δ intrinsic quadrupole moment

$$Q_0 = \frac{4}{3}\left\langle \sum_{k=1}^{Z} r_k^2 \right\rangle \delta$$

uniformly-charged spheroidal nucleus
with a sharp surface

$$\delta = \frac{3}{2}\frac{(R_3)^2 - (R_\perp)^2}{(R_3)^2 + 2(R_\perp)^2}$$

β or β_2 β_2 is defined in terms of the expansion of the density distribution in spherical harmonics.

radius $$R(\theta,\varphi) = R_0(1 + \beta_2 Y_{20}^{\ *}(\theta) + ...)$$

density $$\rho(\vec{r}) = \rho_0(r) - R_0 \frac{\partial \rho_0}{\partial r}(\beta_2 Y_{20}^{*}(\theta) + ...)$$

δ_{osc} or ε In the deformed harmonic oscillator model it is customary to use

$$\varepsilon \ = \ \delta_{osc} \equiv 3\frac{\omega_\perp - \omega_3}{2\omega_\perp + \omega_3} \approx \frac{R_3 - R_\perp}{R_{av}}$$

To leading order, $\delta \approx \beta_2 \approx \delta_{osc}$, but ....

$\delta_n \approx \delta_p$ for stable nuclei, but $\delta_n < \delta_p$ possibly for neutron-rich nuclei towards the neutron-drip-line, since $R_n > R_p$ $\because)$ $R_n\delta_n \approx R_p\delta_p$: displacement of the surface

Nuclei with deformed ground state close to the β stability line

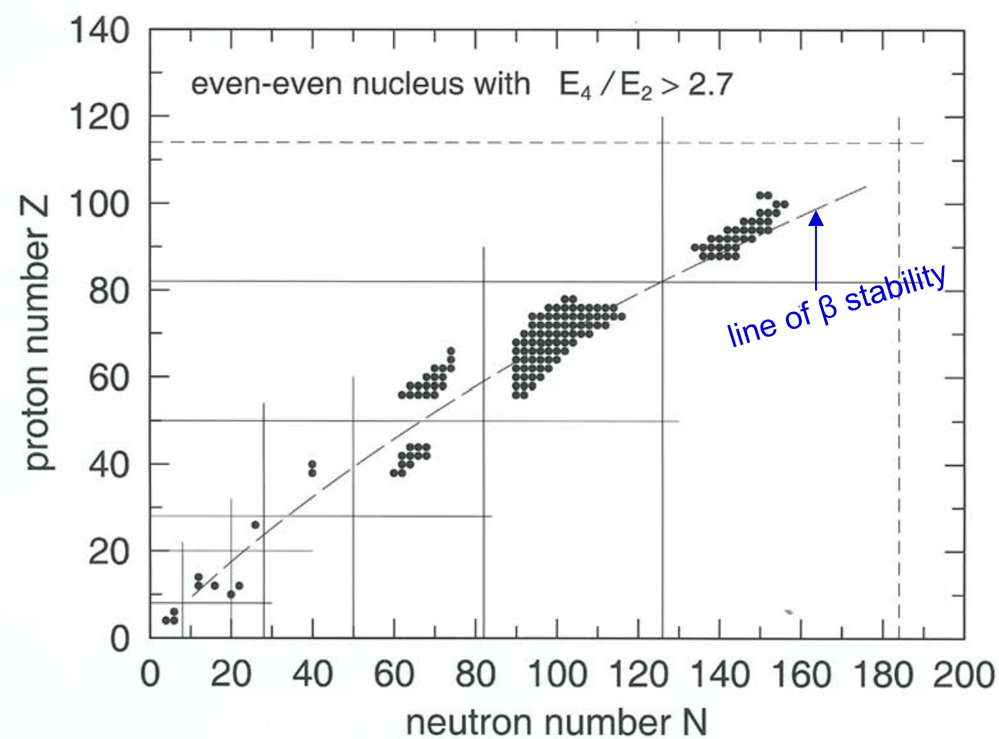

Region of deformed even-even nuclei

All stable single or double closed-shell nuclei are spherical.

some typical examples of deformed nuclei :

$^{12}C_6$ Oblate (pancake shape)

$^{24}Mg_{12}$ Prolate (cigar shape)

rare-earth nuclei with

$90 \leq N \leq 112$

mostly prolate

Some new region of deformed ground-state nuclei away from β stability line;

1) N ≈ Z ≈ 38 ex. $^{72}_{36}Kr_{36}$ (oblate ?) $^{76}_{38}Sr_{38}$ (prolate ?) $^{80}_{40}Zr_{40}$ (prolate ?)

2) N ≈ 20 ex. $^{30}_{10}Ne_{20}$ $^{32}_{10}Ne_{22}$ $^{32}_{12}Mg_{20}$ $^{34}_{12}Mg_{22}$ ("island of inversion")

3) N ≈ 8 ex. $^{11}_{4}Be_7$ $^{12}_{4}Be_8$ $^{14}_{4}Be_{10}$

etc.

Deformed ground state of $N \approx Z$ nuclei (proton-rich compared with stable nuclei)

Coexistence of prolate and oblate shape :

(Z=36)

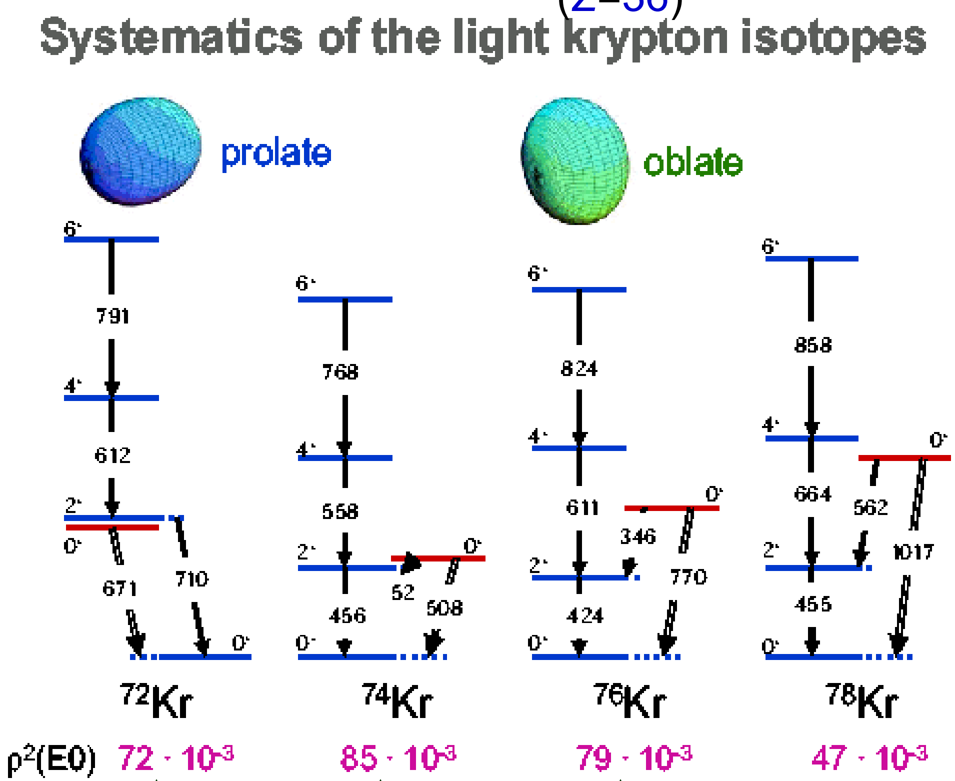

Shape of the ground state (from Coulomb excitation);

oblate prolate prolate

(A.Goergen, Gammapool workshop in Trento, 2006)

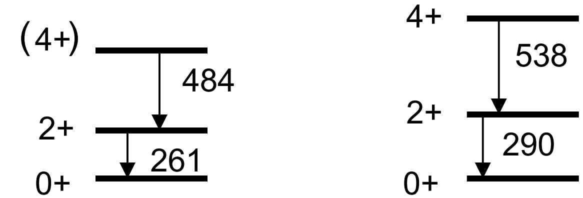

$^{76}_{38}Sr_{38}$ $^{80}_{40}Zr_{40}$

Most probably prolate

OBS. Almost all stable nuclei with N (or Z) = 40 are spherical.

Ex.

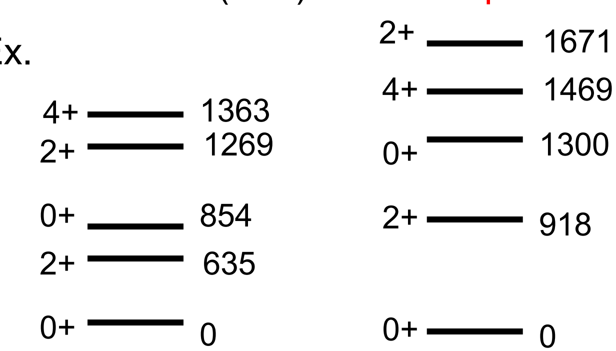

$^{74}_{34}Se_{40}$ $^{94}_{40}Zr_{54}$

S(n) = 504 keV

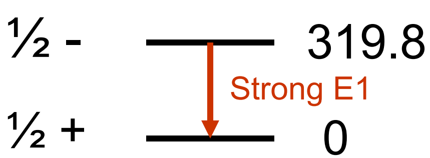

$^{11}_{4}Be_{7}$

The spin-parity of the ground state, ½+ , as well as the small energy distance between the ½ - and ½+ levels, 320 keV, is easily explained, If the nucleus is deformed !

N=8 is not a magic number !
(in this neutron-rich nucleus)

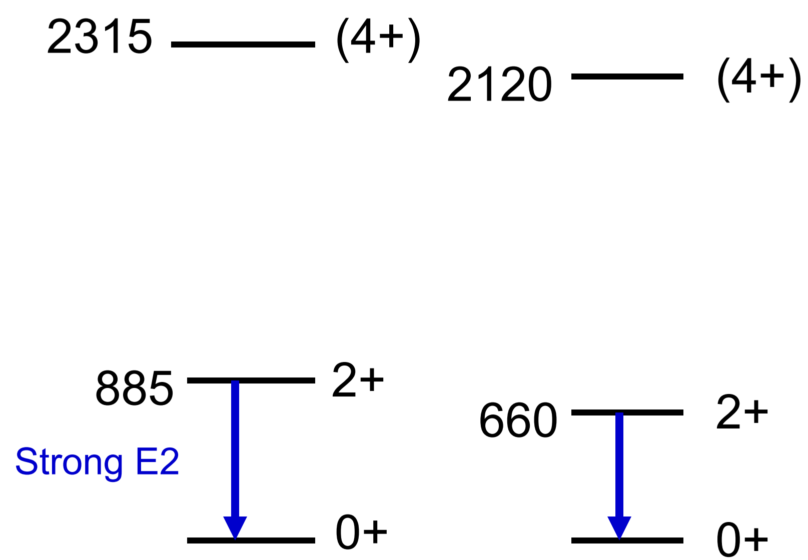

	$^{32}_{12}Mg_{20}$	$^{34}_{12}Mg_{22}$
β =	0.52	0.58
S(n) =	5.81	4.16 MeV
$\frac{E(4+)}{E(2+)}$ =	(2.62)	(3.21)

N=20 is not a magic number !
(in these neutron-rich nuclei)

Example of deformed excited states of magic nuclei

${}^{40}_{20}Ca_{20}$: doubly-magic nucleus, spherical ground state

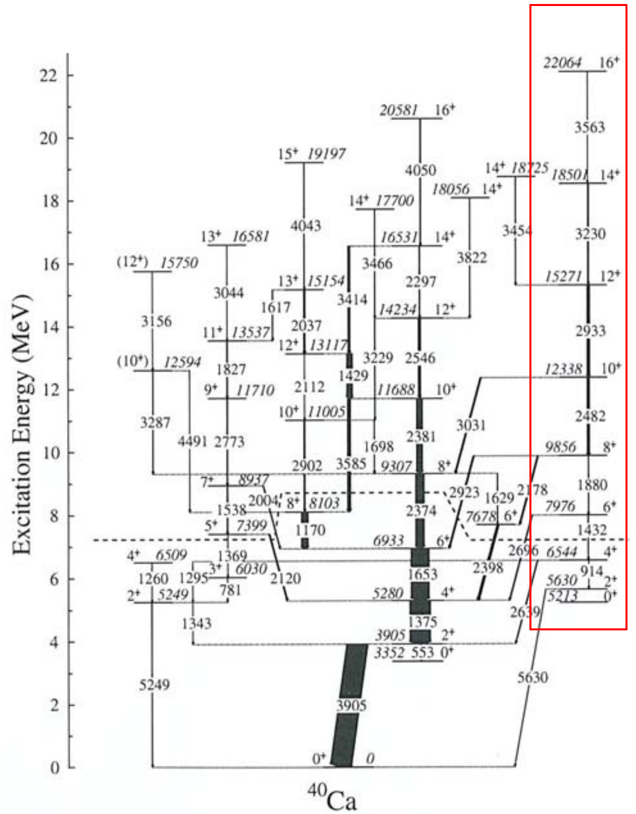

FIG. 1. Partial level scheme of ^{40}Ca; the energy labels are

strongly-deformed band

$Q_t = 1.80 \begin{array}{l} +0.39 \\ -0.29 \end{array}$ eb

from Doppler shift measurement

$\longrightarrow \quad \beta = 0.59 \begin{array}{l} +0.11 \\ -0.07 \end{array}$

From E.Ideguchi et al., Phys.Rev.Lett. 87 (2001) 222501.

Implication of rotational spectra :

(1) Existence of deformation (in the body-fixed system), so as to specify an orientation of the system as a whole.

(2) Collective rotation, as a whole, and internal motion w.r.t. the body-fixed system are approximately separated in the complicated many-body system.

Classical system : An infinitesimal deformation is sufficient to establish anisotropy.

Quantum system : [zero-point fluctuation of deformation] << [equilibrium deformation], in order to have a well-defined rotation.

Indeed,

collective rotation is the best established collective motion in nuclei.

For some nuclei Hartree-Fock (HF) calculations with rotationally-invariant Hamiltonian end up with a deformed shape !

$\begin{cases} \text{spherical shape} \leftarrow \text{HF solutions for "closed-shell" nuclei} \\ \text{deformed shape} \leftarrow \text{HF solutions for some nuclei} \end{cases}$

exhibit rotational spectra

∴ Deformed shape obtained from HF calculations is interpreted as the intrinsic shape in the body-fixed system.

The notion of one-particle (or one-quasiparticle if pair correlation is included) motion in deformed nuclei can be much more widely, in a good approximation, applicable than in spherical nuclei.

∵) The major part of the long-range two-body interaction is already taken into account in the deformed mean-field.

Thus, the spectroscopy of deformed nuclei is often much simpler than that of spherical vibrating nuclei.

What can one learn from observed rotational spectra ?

(a) Quantum numbers of rotational spectra $\leftrightarrow$ symmetry of deformation

ex. Parity is a good quantum number $\leftarrow$ space reflection invariance,
K is a good quantum number $\leftarrow$ Axially-symmetric shape ($E(I) \propto I(I+1)$) ,
where K is the projection of angular momentum along the symmetry axis.
The $K^{\pi}=0^{+}$ ground band has only I = 0, 2,4,… $\leftarrow$ shape is *R*- invariant,
Kramers degeneracy $\leftarrow$ time reversal invariance,
etc.

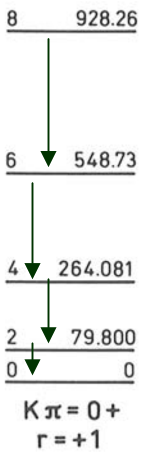

(b) rotational energy, E(I) - E(I-2)
E2 transition probability $\downarrow$ } $\leftrightarrow$ size of deformation

---

R-invariant shape : in addition to axially-symmetry, the shape is further invariant w.r.t. a rotation of π about an axis perpendicular to the symmetry axis.
(If a shape is already axial symmetric, reflection invariance is equivalent to *R*-inv.)
ex. Y_{20} deformed shape is *R*-invariant, but not Y_{30} deformed (pear) shape.

Kramers degeneracy : The levels in an odd-fermion system are at least doubly degenerate.

Pause: Appearance of only even (or odd) angular momenta

Coming from the *R*-symmetry of Y_{20} deformation (or $Y_{\lambda 0}$ deformation with even λ) ;

The ground-state (pairwise levels, Ω and –Ω, are occupied) of Y_{20} deformed even-even nuclei ($K^{\pi} = 0^{+}$) has r (eigenvalue of *R*-operation) = +1 and, thus, the rotational-band has members with $I^{\pi} = 0^{+}, 2^{+}, 4^{+}, 6^{+}, \ldots\ldots$

The rotational band based on excited $K^{\pi} = 0^{-}$ configurations may have either

r = –1 with members $I^{\pi} = 1^{-}, 3^{-}, 5^{-}, \ldots\ldots$

that has been often observed in medium-heavy deformed nuclei

or

r = +1 with members $I^{\pi} = 0^{-}, 2^{-}, 4^{-}, \ldots\ldots$

OBS. The rotational bands based on intrinsic configurations with $K^{\pi} = 1^{-}$ have members $I^{\pi} = 1^{-}, 2^{-}, 3^{-}, 4^{-}, 5^{-}, \ldots\ldots$

Coming from the (Fermion or Boson) statistics ;

The two-fermion system in a j-shell (j : half integer) has only even total angular momentum,

$(j^2)_J$ where J is an even integer.

The two-phonon system with the same phonon (λ : integer) has only even total angular momentum,

$(\lambda^2)_J$ where J is an even integer.

Why are some nuclei deformed ?

Usual understanding ;

Deformation of ground states (ND, $R_{\perp} : R_z \approx 1 : 1.3$) $\leftarrow$ Jahn-Teller effect

Many particles outside a closed shell in a spherical potential
$\rightarrow$ near degeneracy in one-particle quantum spectra
$\rightarrow$ possibility of gaining energy by breaking away from spherical symmetry using the degeneracy.

Weakly-bound nuclei
$\rightarrow$ possible change of shell-structure
$\rightarrow$ near degeneracy in one-particle spectra at neutron numbers different from stable nuclei.

Superdeformation (SD, $R_{\perp} : R_z \approx 1 : 2$) at high spins in rare-earth nuclei or fission isomers in actinide nuclei
$\leftarrow$ new shell structure (and new magic numbers !) at large deformation

3.2. Important deformation and quantum numbers in deformed nuclei

Axially symmetric quadrupole (Y_{20}) deformation (that has *R*-symmetry)

\- most important deformation in nuclei

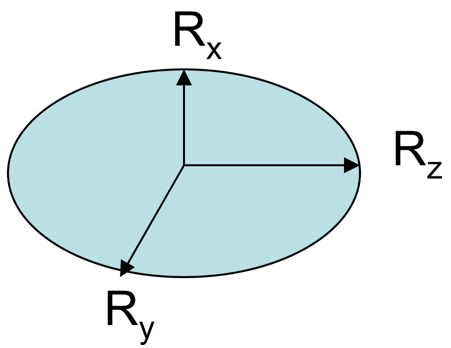

z-axis = symmetry axis

$R_\perp (= R_x = R_y) < R_z$ prolate (cigar shape)

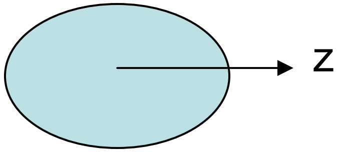

$R_\perp (= R_x = R_y) > R_z$ oblate (pancake shape)

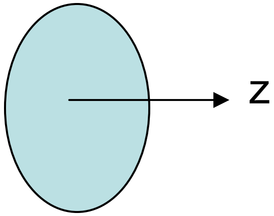

One-particle Hamiltonian with spin-orbit potential

$$H = T + V(r,\theta)$$

$$V(r,\theta) = V_0(r) + V_2(r) Y_{20}(\theta) + V_{\ell s}(r)(\vec{\ell} \cdot \vec{s}) \qquad Y_{20}(\theta) = \sqrt{\frac{5}{16\pi}}(3\cos^2\theta - 1)$$

where θ is polar angle w.r.t. the symmetry axis (= z-axis)

Quantum numbers of one-particle motion in H

(1) Parity $\pi = (-1)^{\ell}$ where ℓ is orbital angular momentum of one-particle.

(2) $\Omega \leftarrow \ell_z + s_z$ $\qquad \because)$

$[\, V_2(r)\, Y_{20}(\theta)\, ,\, \ell_z + s_z\,] = 0$ and $\left[(\vec{\ell} \cdot \vec{s}), \ell_z + s_z\right] = 0$

4. One-particle motion well-bound in Y_{20} deformed potential

4.1. Limits of small and large deformation

$$V(r,\theta) = V_0(r) + \underline{V_2(r)Y_{20}(\theta)} + \underline{V_{\ell s}(r)(\vec{\ell}\cdot\vec{s})}$$

Small deformation and/or high-j orbits

$$\boxed{\langle V_2(r)Y_{20}(\theta)\rangle << \langle V_{\ell s}(r)(\vec{\ell}\cdot\vec{s})\rangle}$$

those pushed down by $(\vec{\ell}\cdot\vec{s})$ potential : ex. $g_{9/2}$, $h_{11/2}$, $i_{13/2}$, ...

Single j-shell :

j (= one-particle angular momentum) is (approximately) a good quantum number.

Ω = ± j, ± (j–1), ….., ±½ : symmetry-axis component of j

$$\langle \ell j \Omega_1 | \beta Y_{20} | \ell j \Omega_2 \rangle \neq 0 \qquad \text{only for} \quad \Omega_1 = \Omega_2$$

$\therefore$

In the linear order of β, the Y_{20} deformation only shifts (∝ β) the energy of doubly-degenerate one-particle states with ± Ω .
One-particle wave-functions remain the same for β ≠ 0.

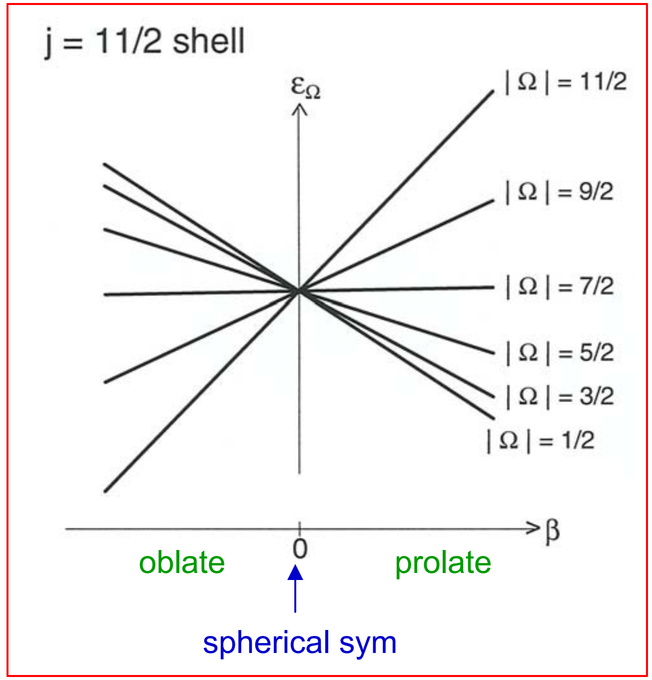

spherical : (2j+1) degeneracy

→ Y_{20} deformed : ± Ω degeneracy

Large (or realistic) deformation

$$\langle V_2(r) Y_{20}(\theta) \rangle >> \langle V_{\ell s}(r)(\vec{\ell} \cdot \vec{s}) \rangle$$

Many j-shells coupled by Y_{20} deformation

$$\langle \ell_1 j_1 \Omega_1 | f(r) Y_{20} | \ell_2 j_2 \Omega_2 \rangle \neq 0 \quad \text{for} \quad \begin{cases} (-1)^{\ell_1} = (-1)^{\ell_2} \\ \Omega_1 = \Omega_2 \\ |j_1 - j_2| \leq 2 \end{cases}$$

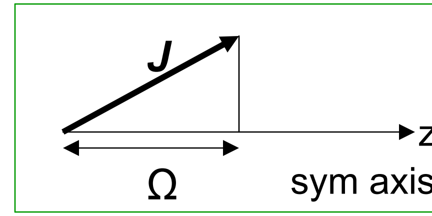

That means, in a Y_{20} deformed mean field with spin-orbit potential

(One-particle angular-momentum j is not a good quantum-number. *$[H, j] \neq 0$*)

Ω : projection of one-particle angular-momentum along the symmetry axis, and a good quantum-number $\quad [H, J_z] = [Y_{20}, J_z] = 0 \quad \Omega \leftarrow J_z = L_z + s_z$

π : parity $\equiv (-1)^{\ell}$

are good quantum-numbers.

For example,

$\Omega^\pi = 1/2^+$ $\quad s_{1/2}$, $d_{3/2}$, $d_{5/2}$, $g_{7/2}$, $g_{9/2}$, ….., components $\quad \ell_{min} = 0$

$\Omega^\pi = 3/2^+$ $\quad d_{3/2}$, $d_{5/2}$, $g_{7/2}$, $g_{9/2}$, $i_{11/2}$ ….., components $\quad \ell_{min} = 2$

$\Omega^\pi = 1/2^-$ $\quad p_{1/2}$, $p_{3/2}$, $f_{5/2}$, $f_{7/2}$, $h_{9/2}$, ….., components $\quad \ell_{min} = 1$

$\Omega^\pi = 3/2^-$ $\quad p_{3/2}$, $f_{5/2}$, $f_{7/2}$, $h_{9/2}$, $h_{11/2}$, ….., components $\quad \ell_{min} = 1$

Y_{20} deformed harmonic-oscillator potential

$$\boxed{\langle V_2(r)Y_{20}(\theta)\rangle >> \langle V_{\ell s}(r)(\vec{\ell}\cdot\vec{s})\rangle}$$

$$V_{def.h.o.} = \frac{M}{2}\left(\omega_z^2 z^2 + \omega_\perp^2 (x^2+y^2)\right)$$

One-particle energy (ε(N) at δ=0 splits into (N+1) levels). ∵) $n_z = 0, 1, \ldots\ldots, N$ where $N = n_z + n_\perp$

$$\varepsilon(n_\perp, n_z) = \left(n_z + \frac{1}{2}\right)\hbar\omega_z + (n_\perp + 1)\hbar\omega_\perp \quad = \quad \hbar\varpi\left(N + \frac{3}{2} - \frac{\delta}{3}(3n_z - N)\right)$$

$$\boxed{\delta \approx \beta}$$

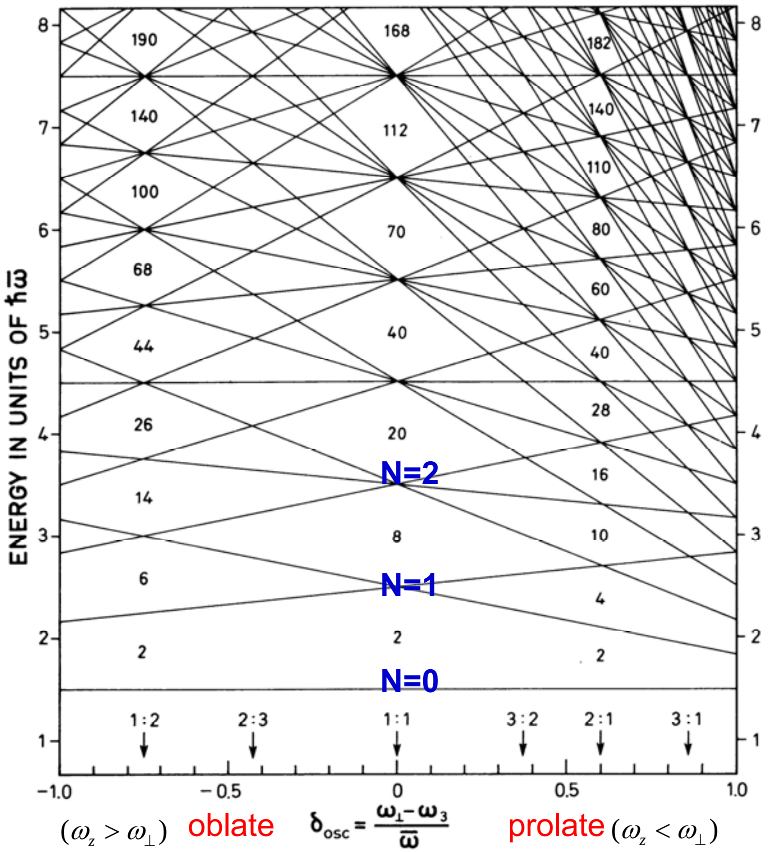

Figure 6-48 Single-particle spectrum for axially symmetric harmonic oscillator potentials.

spherical sym

where

$$n_\perp = n_x + n_y \qquad N = n_x + n_y + n_z$$

$$\varpi \equiv \frac{1}{3}(\omega_z + 2\omega_\perp) \qquad \delta \equiv 3\frac{\omega_\perp - \omega_z}{2\omega_\perp + \omega_z} \approx \frac{R_z - R_\perp}{R_{av}}$$

$\varepsilon(n_\perp, n_z)$ has $\underline{2(n_\perp + 1)}$ degeneracy.

spin ↑↓

$n_x = 0, 1, \ldots\ldots, n_\perp$

Denote one-particle energies by $[n_x\, n_y\, n_z]$ or

$[N\, n_z\, n_x]$ or $[N\, n_z\, \Lambda]$ (cf. $[V_{def.h.o.}, L_z] = 0$

Λ $(\Leftarrow L_z) = \pm n_\perp, \pm(n_\perp - 2), \ldots\ldots,$ ±1 or 0

Asymptotic quantum numbers including spin (= ½)

$\boxed{[\, N\, n_z\, \Lambda\, \Omega]}$ where $\Lambda > 0$, $\Omega \Leftarrow L_z + s_z$

$= \Lambda \pm ½ > 0$

$$\omega_z^2 z^2 + \omega_\perp^2 (x^2+y^2)$$

$$= \frac{1}{3}\left(\omega_z^2 + 2\omega_\perp^2\right)\underbrace{\left(x^2+y^2+z^2\right)}_{r^2} + \frac{1}{3}\left(\omega_z^2 - \omega_\perp^2\right)\underbrace{\left(2z^2-(x^2+y^2)\right)}_{\sqrt{\frac{16\pi}{5}}\, r^2 Y_{20}(\theta)}$$

$$\approx \quad f(r) + c\,\delta\, r^2\, Y_{20}(\theta) \qquad \text{up till } O(\delta)$$

---

h.o. potential :

- no surface – maybe applicable for strongly bound system
- no spin-orbit potential – maybe applicable for large deformation

---

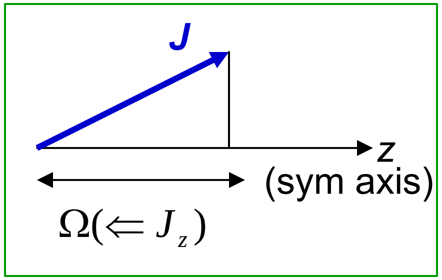

One-particle levels in axially-symmetric quadrupole (Y_{20}) deformation

(prolate or oblate shape) are denoted by

$\boxed{[N\ n_z\ \Lambda\ \Omega]}$: asymptotic quantum-numbers. $\Lambda(\Leftarrow L_z)$ with $\Omega > 0$ and $\Lambda > 0$

where Ω and parity $\pi = (-1)^{\ell} = (-1)^N$ is a good quantum-number.

One-particle energy is degenerate for $\pm\Omega$

One-particle levels for a finite quadrupole deformation β are often denoted by $[N\ n_z\ \Lambda\ \Omega]$, since for $|\beta|>0.3$ the wave functions are approximately expressed by $[N\ n_z\ \Lambda\ \Omega]$, except high-j orbits.

4.2. "Nilsson diagram" – one-particle spectra as a function of deformation

Ex. [harmonic-oscillator + surface effect + spin-orbit] potential = [modified oscillator] potential

Doubly-degenerate ($\pm\,\Omega$) one-particle levels are denoted by

asymptotic quantum numbers $[N\ n_z\,\Lambda\ \Omega]$ with $\Lambda,\ \Omega > 0$,

which become good quantum numbers for very large $|\beta|$.

$N = n_z + n_\perp$

$\Lambda(>0) = n_\perp,\ n_\perp - 2,\ \ldots, 1 \text{ or } 0$

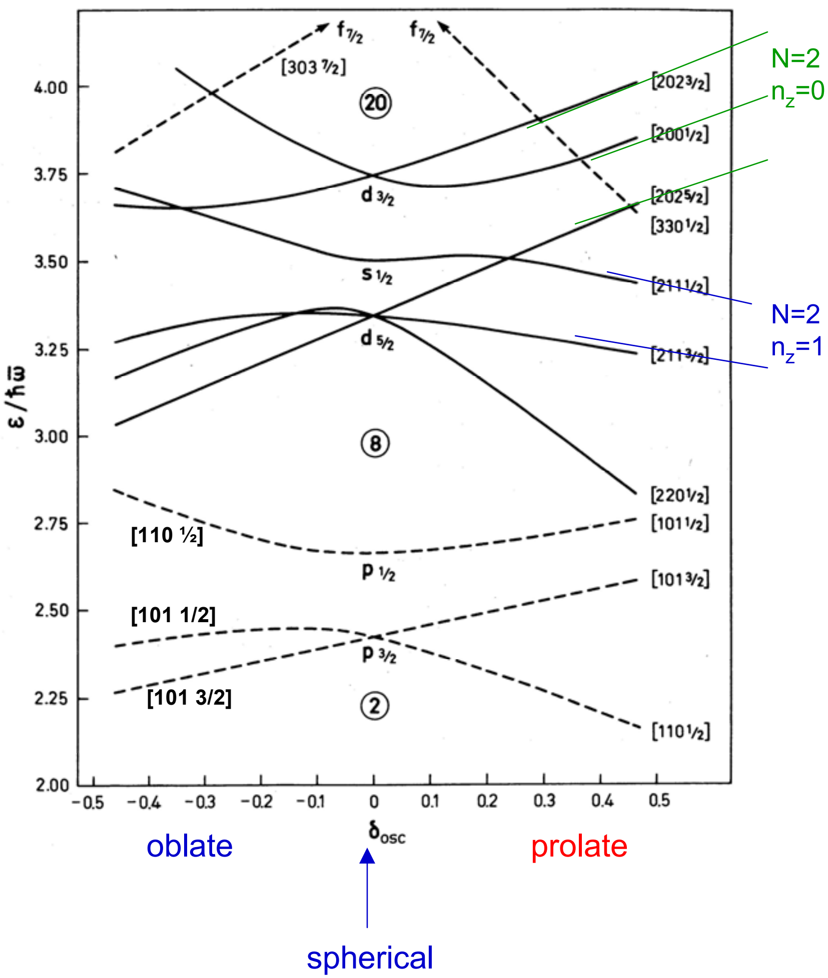

For $\beta\ (\sim\delta) > 0$ (prolate shape)

1) [prolate] For a given N : $\varepsilon_\Omega \rightarrow$ lower for $n_z \rightarrow$ larger

ex. Nilsson levels in sd-shell (N=2)

$\Omega^\pi = 1/2^+$	$\Omega^\pi = 3/2^+$	$\Omega^\pi = 5/2^+$
[200 1/2] [211 1/2] [220 1/2]	[202 3/2] [211 3/2]	[202 5/2]

ε

2) [surface] For given $\{N, n_z\}$: $\varepsilon_\Omega \rightarrow$ lower for $\Lambda \rightarrow$ larger

3) [spin-orbit] For given $\{N, n_z, \Lambda\}$: $\varepsilon_\Omega \rightarrow$ lower for $\Omega \rightarrow$ larger

---

At large β ($\sim\delta$), $\quad \varepsilon \propto -\delta(3n_z - N)$

i.e. ε as a function of β depends only on $\beta(3n_z - N)$

Proton orbits in prolate potential ($50 < Z < 82$).

$g_{7/2}$, $d_{5/2}$, $d_{3/2}$ and $s_{1/2}$ orbits, which have $\pi = +$, do not mix with $h_{11/2}$ by Y_{20} deformation.

[N=4, n_z =0]

$h_{11/2}$ orbit
= high-j orbit
with π = –

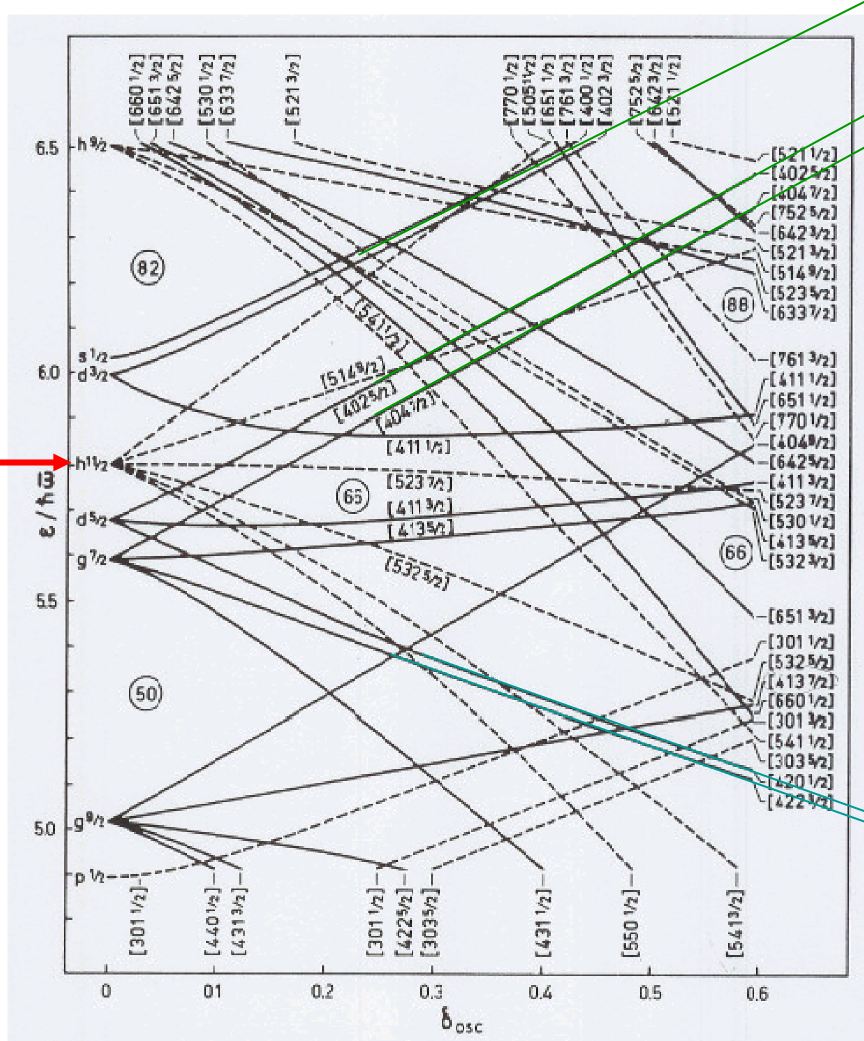

Figure 5-2 Proton orbits in prolate potential ($50 < Z < 82$). The spectra in this and the

[N=4, n_z =2]

Levels are doubly degenerate with $\pm\,\Omega$.

At small δ and $h_{11/2}$ orbit,

$$\varepsilon \ \propto \ \delta\,(3\Omega^2 - j(j+1)\,)$$

At large δ,

$$\varepsilon \ \propto \ -\,\delta(3n_z - N)$$

At δ > 0.3 for prolate shape quantum numbers [$Nn_z\Lambda\Omega$] work well, except for high-j orbits.

Table 1.

Ex.1. Deformed one-particle wave-functions denoted by the asymptotic quantum numbers $[N\ n_z\ \Lambda\ \Omega]$ are expanded in terms of spherical basis.
(A modified-oscillator Hamiltonian was diagonalized.)

$[Nn_3\Lambda\Omega]$	$j=1/2$	$j=3/2$	$j=5/2$	$j=7/2$
[101 1/2]	0.920	0.392		
[220 1/2]	−0.523	−0.285	0.803	
[211 3/2]		−0.236	0.972	
[202 5/2]			1.000	
[211 1/2]	0.419	0.735	0.533	
[200 1/2]	0.743	−0.615	0.265	
[202 3/2]		0.972	0.236	
[330 1/2]	0.279	−0.646	−0.188	0.685

Table 5-9 Single-particle wave functions for nuclei with $19 \leqslant A \leqslant 25$. The table gives the expansion coefficients $\langle Nlj\Omega|\nu\rangle$ of the one-particle orbits ν labeled by the asymptotic quantum numbers $[Nn_3\Lambda\Omega]$. The wave functions are obtained from the Hamiltonian (5-10) employing the parameters of Table 5-1 and the deformation $\delta=0.4$. The phases are as in Table 5-2b and Eq. (5-17).

parity of the states: $\pi = (-1)^N = (-1)^\ell$

OBS. Various computer programs are at present publicly available if one is satisfied with the diagonalization of modified-oscillator Hamiltonian.

Table 1. (continued)

Ex.2. Using Tables 5-2a and 5-2b in A.Bohr and B.R.Mottelson, Nuclear Structure, vol.II, one obtains, for example,

Normal-parity orbits;

$$| [411\ 3/2] \rangle = 0.926\, | 411\ 3/2 \rangle + \dots$$
$$= 0.418\, |g_{9/2}\rangle - 0.140\, |g_{7/2}\rangle + 0.864\, |d_{5/2}\rangle + 0.246\, |d_{3/2}\rangle$$

$$| [411\ 1/2] \rangle = 0.900\, | 411\ 1/2 \rangle + \dots$$
$$= -0.163\, |g_{9/2}\rangle + 0.396\, |g_{7/2}\rangle - 0.099\, |d_{5/2}\rangle + 0.848\, |d_{3/2}\rangle + 0.297 |s_{1/2}\rangle$$

$$| [400\ 1/2] \rangle = 0.968\, | 400\ 1/2 \rangle + \dots$$
$$= 0.147\, |g_{9/2}\rangle - 0.072\, |g_{7/2}\rangle + 0.539\, |d_{5/2}\rangle - 0.160\, |d_{3/2}\rangle + 0.811\, |s_{1/2}\rangle$$

High-j orbits;

$$| [532\ 5/2] \rangle = 0.861\, | 532\ 5/2 \rangle + \dots$$
$$= 0.882\, |h_{11/2}\rangle + 0.339\, |h_{9/2}\rangle - 0.244\, |f_{7/2}\rangle - 0.062\, |f_{5/2}\rangle$$

for proton one-particle wave-functions at deformation $\delta = 0.3$, which are obtained by diagonalizing a modified-oscillator Hamiltonian,

$H = T + V(r,\theta)$ plus $(\boldsymbol{\ell}\cdot\boldsymbol{s})$ potential

OBS.

$| [411\ 3/2] \rangle$: states obtained by diagonalization

$| 411\ 3/2 \rangle$: bases states exactly expressed by the quantum numbers $N\ n_z\ \Lambda\ \Omega$

Intrinsic configuration in the body-fixed system

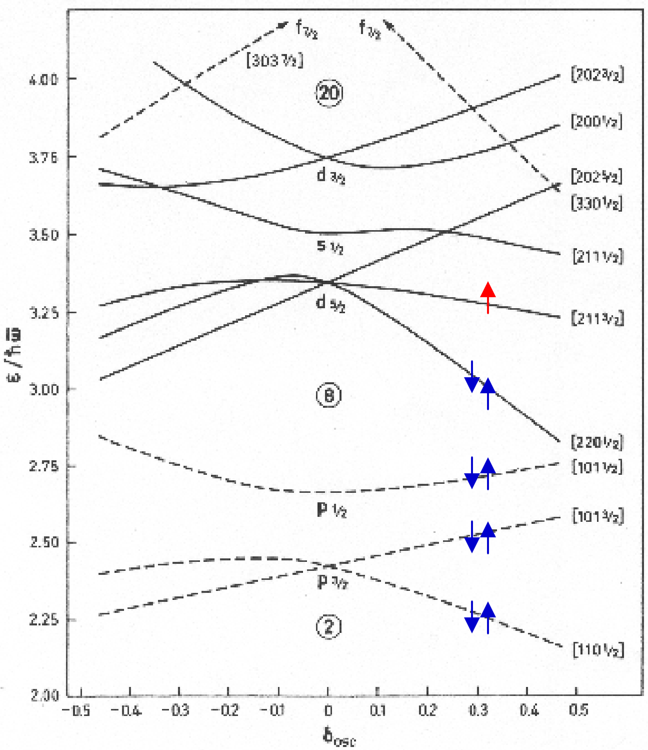

Good approximation ;

(a) In the ground state of eve-even nuclei

$$K \equiv \sum_{i=1}^{A} \Omega_i = 0$$

Namely, ± Ω levels are pairwise occupied.

(b) In low-lying states of odd-A nuclei

$$K \equiv \sum_{i=1}^{A} \Omega_i \quad \Rightarrow \quad \Omega \text{ of the last unpaired particle.}$$

Low-lying rotational bands in deformed odd-A nuclei may well be classified in terms of one-particle orbit $[Nn_z \Lambda\Omega]$ occupied by the last unpaired particle.

The rotational band based on $[N\ n_z\ \Lambda\ \Omega]$

(a) $I \geq K\ (\leftarrow I_3) = \Omega$

(b) the bandhead state has I=K.
Exception may occur for K=1/2 bands.

(c) some irregular rotational spectra are observed for K=1/2 bands.

ex. The N=13 th neutron orbits observed as low-lying excitations in $^{25}Mg_{13}$ - a textbook example

[N n $_z$ Λ Ω]

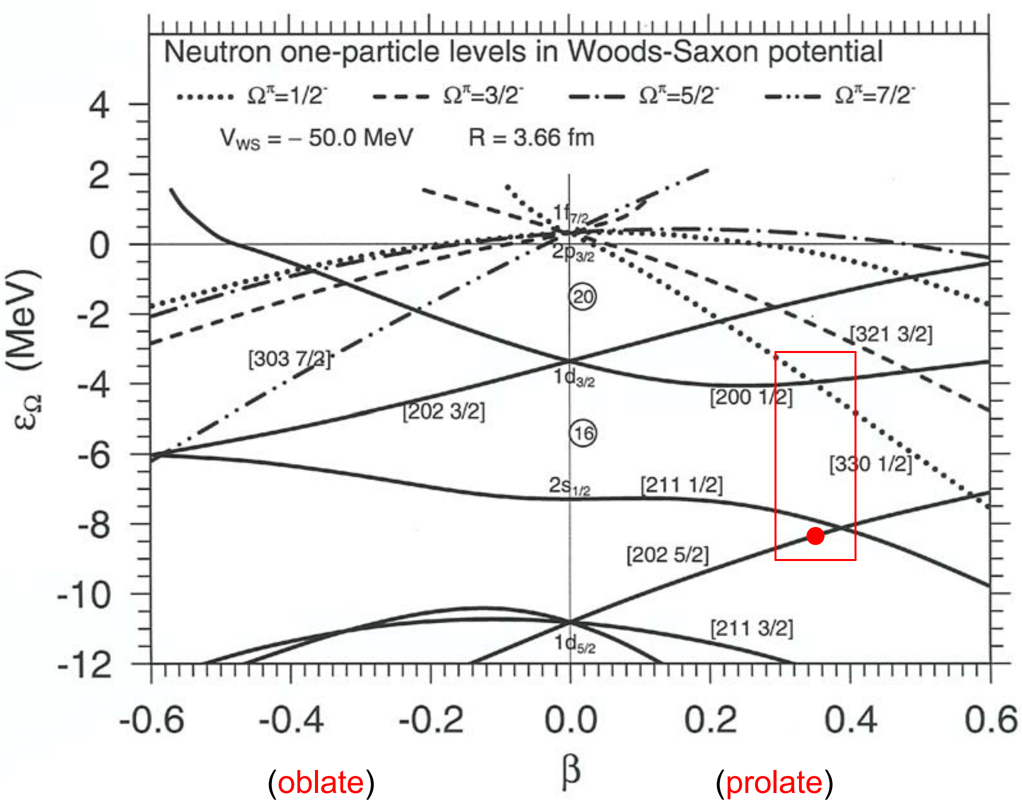

Bohr & Mottelson, Nuclear Structure, Vol.II

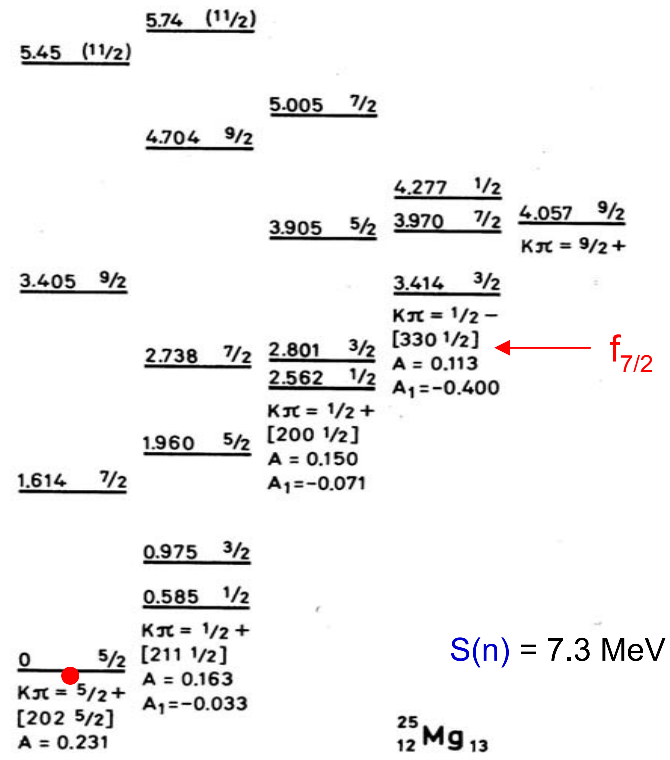

Nilsson levels : double (±Ω) degeneracy

The above interpretation of the data works quantitatively :

measured large E2 transitions within the bands

$\rightarrow$ $\beta \approx 0.4$

observed E2- and M1-intensity relations

$\rightarrow$ $g_s^{eff} = (0.7 – 0.9)\ g_s^{free}$

Some selection rules in terms of exact quantum numbers, I, K, or $N\, n_z\, \Lambda\, \Omega$

(More complete formulas are given in Table 2.)

1) Between states (I, K) and (I', K')

$E\lambda$ or $M\lambda$ transitions are forbidden for $|I - I'| > \lambda$

$E\lambda$ or $M\lambda$ transitions are forbidden for $|K - K'| > \lambda$, even if $|I - I'| \leq \lambda$

("*K*-selection rule")

2) Noting that *M1* $\propto \vec{\ell}$ or $\vec{s}$, and *GT* $\propto \vec{s}$

$$(\ell_x \pm i\ell_y)\,|Nn_z\Lambda\Omega\rangle \quad \propto \quad |N, n_z+1, \Lambda\pm1, \Omega\pm1\rangle \quad \text{or} \quad \propto \quad |N, n_z-1, \Lambda\pm1, \Omega\pm1\rangle$$

$$\ell_z\,|Nn_z\Lambda\Omega\rangle \quad = \quad \Lambda\,|Nn_z\Lambda\Omega\rangle$$

$$(s_x \pm is_y)\,|Nn_z\Lambda\Omega\rangle \quad = \quad \left[\left(\frac{1}{2}\mp\Sigma\right)\left(\frac{1}{2}\pm\Sigma+1\right)\right]^{1/2}\,|N, n_z, \Lambda, \Omega\pm1\rangle$$

$$s_z\,|Nn_z\Lambda\Omega\rangle \quad = \quad \Sigma\,|Nn_z\Lambda\Omega\rangle$$

where

$s_z \longrightarrow \Sigma = \Omega - \Lambda$

How well "*K*-selection rule" of 1) works in reality exhibits how good axial symmetry is.

The selection rules in 2) approximately work for transitions between realistic one-particle states, $[N\, n_z\, \Lambda\, \Omega]$ and $[N'\, n_z'\, \Lambda'\, \Omega']$, if $\beta > 0.3$

Table 2.

Selection rule of one-particle operators between one-particle states with exact quantum numbers, $N\ n_z\ \Lambda\ \Omega$.

Matrix elements of the most important operators in the asymptotic basis, and their selection rules

Operator O	ΔN	ΔN_z	$\Delta\Lambda$	$\Delta\Sigma$	$\Delta\Omega$	$\langle N'N'_z\Lambda' \vert O \vert NN_z\Lambda\rangle$
	0	0	0	0	0	$\Lambda\Sigma$
$l_t \cdot s$	0	1	±1	∓1	0	$-\frac{1}{2}(\frac{1}{2}\pm\Sigma)\,[(N_z+1)\,(N-N_z\mp\Lambda)]^{\frac{1}{2}}$
	0	-1	±1	∓1	0	$-\frac{1}{2}(\frac{1}{2}\pm\Sigma)\,[N_z\,(N-N_z\pm\Lambda+2)]^{\frac{1}{2}}$
	0	0	0	0	0	$\Lambda^2+\Lambda+2\,[N_z\,(N-N_z+1)]+(N-N_z-\Lambda)$
l_t^2	0	2	0	0	0	$[(N_z+1)\,(N_z+2)\,(N-N_z+\Lambda)\,(N-N_z-\Lambda)]^{\frac{1}{2}}$
	0	-2	0	0	0	$[N_z\,(N_z-1)\,(N-N_z\mp\Lambda+2)\,(N-N_z-\Lambda+2)]^{\frac{1}{2}}$
z'	±1	±1	0	0	0	$c_z\,[\frac{1}{2}(N_z\,\mathrm{sup})]^{\frac{1}{2}}$
$x'\pm iy'$	$+1$	0	±1	0	±1	$\pm c_\perp\,[\frac{1}{2}(N-N_z\pm\Lambda+2)]^{\frac{1}{2}}$
	-1	0	±1	0	±1	$\mp c_\perp\,[\frac{1}{2}(N-N_z\mp\Lambda)]^{\frac{1}{2}}$
	0	0	0	0	0	$c_z^2\,(N_z+\frac{1}{2})$
z'^2	2	2	0	0	0	$\frac{1}{2}c_z^2\,[(N_z+1)\,(N_z+2)]^{\frac{1}{2}}$
	-2	-2	0	0	0	$\frac{1}{2}c_z^2\,[N_z\,(N_z-1)]^{\frac{1}{2}}$
	0	0	0	0	0	$c_\perp^2\,(N-N_z+1)$
$x'^2+y'^2$	2	0	0	0	0	$-\frac{1}{2}c_\perp^2\,[(N-N_z+\Lambda+2)\,(N-N_z-\Lambda+2)]^{\frac{1}{2}}$
	-2	0	0	0	0	$-\frac{1}{2}c_\perp^2\,[(N-N_z+\Lambda)\,(N-N_z-\Lambda)]^{\frac{1}{2}}$
	0	1	±1	0	±1	$\mp\frac{1}{2}c_\perp c_z\,[(N_z+1)\,(N-N_z\mp\Lambda)]^{\frac{1}{2}}$
$z'(x'\pm iy')$	0	-1	±1	0	±1	$\pm\frac{1}{2}c_\perp c_z\,[N_z\,(N-N_z\pm\Lambda+2)]^{\frac{1}{2}}$
	2	1	±1	0	±1	$\pm\frac{1}{2}c_\perp c_z\,[(N_z+1)\,(N-N_z\pm\Lambda+2)]^{\frac{1}{2}}$
	-2	-1	±1	0	±1	$\mp\frac{1}{2}c_\perp c_z\,[N_z\,(N-N_z\mp\Lambda)]^{\frac{1}{2}}$
	0	0	±2	0	±2	$-c_\perp^2\,[(N-N_z\mp\Lambda)\,(N-N_z\pm\Lambda+2)]^{\frac{1}{2}}$
$(x'\pm iy')^2$	2	0	±2	0	±2	$\frac{1}{2}c_\perp^2\,[(N-N_z\pm\Lambda+2)\,(N-N_z\pm\Lambda+4)]^{\frac{1}{2}}$
	-2	0	±2	0	±2	$\frac{1}{2}c_\perp^2\,[(N-N_z\mp\Lambda)\,(N-N_z\mp\Lambda-2)]^{\frac{1}{2}}$
l_z	0	0	0	0	0	Λ
	0	1	±1	0	±1	$-\mathscr{S}\,[(N_z+1)\,(N-N_z\mp\Lambda)]^{\frac{1}{2}}$
$l_x\pm il_y$	0	-1	±1	0	±1	$-\mathscr{S}\,[N_z\,(N-N_z\pm\Lambda+2)]^{\frac{1}{2}}$
	2	1	±1	0	±1	$\mathscr{D}\,[(N_z+1)\,(N-N_z\pm\Lambda+2)]^{\frac{1}{2}}$
	-2	-1	±1	0	±1	$\mathscr{D}\,[N_z\,(N-N_z\mp\Lambda)]^{\frac{1}{2}}$
s_z	0	0	0	0	0	Σ
$s_x\pm is_y$	0	0	0	±1	±1	$[(\frac{1}{2}\mp\Sigma)\,(\frac{1}{2}\pm\Sigma+1)]^{\frac{1}{2}}$

E1 operator

E2 operator

M1 operator

Gamow-Teller operator

The matrix elements between realistic levels with the assigned asymptotic quantum numbers, $[N\ n_z\ \Lambda\ \Omega]$, can be obtained, to leading order, from this table.

From J.P.Boisson and R.Piepenbring, Nucl. Phys. A168(1971)385.

If you use this kind of tables, you must be careful about the sign of the non-diagonal matrix elements, which depends on the phase convention of wave functions !

Table 3.

$$\left|(\ell s)\,j,\Omega\right\rangle \;\equiv\; \frac{1}{r}R_{\ell j}(r)\sum_{m_\ell m_s} C(\ell,1/2,j;m_\ell m_s\Omega)Y_{\ell m_\ell}(\theta,\phi)\chi_{1/2,m_s}$$

$$\left\langle \ell_2 j_2\left|r^\lambda\right|\ell_1 j_1\right\rangle \;\equiv\; \int_0^\infty dr R_{\ell_2 j_2}(r)R_{\ell_1 j_1}(r)r^\lambda$$

Matrix-elements of one-particle operators in $|(\ell\ s)\ j,\ \Omega\,\rangle$ representations

$$\left\langle(\ell_2 s)\,j_2,\Omega\left|r^\lambda Y_{\lambda 0}\right|(\ell_1 s)\,j_1,\Omega\right\rangle$$

$$= \;\delta\left((-1)^{\ell_1+\ell_2},(-1)^\lambda\right)\left\langle\ell_2 j_2\left|r^\lambda\right|\ell_1 j_1\right\rangle(-1)^{j_1+j_2+1+\lambda}(-1)^{\Omega-\frac{1}{2}}\sqrt{\frac{(2j_1+1)(2j_2+1)}{4\pi(2\lambda+1)}}$$

$$C(j_2 j_1\lambda;1/2,-1/2,0)\;\;C(j_2 j_1\lambda;\Omega,-\Omega,0)$$

$$\left\langle(\ell_2 s)\,j_2,\Omega+1\left|r^\lambda Y_{\lambda 1}\right|(\ell_1 s)\,j_1,\Omega\right\rangle$$

$$= \;\delta\left((-1)^{\ell_1+\ell_2},(-1)^\lambda\right)\left\langle\ell_2 j_2\left|r^\lambda\right|\ell_1 j_1\right\rangle(-1)^{j_1+j_2+1+\lambda}(-1)^{\Omega-1/2}\sqrt{\frac{(2j_1+1)(2j_2+1)}{4\pi(2\lambda+1)}}$$

$$C(j_2 j_1\lambda;1/2,-1/2,0)\;\;\;C(j_2 j_1\lambda;\Omega+1,-\Omega,1)$$

$$= \;\;(-1)\left\langle(\ell_1 s)\,j_1,\Omega\left|r^\lambda Y_{\lambda-1}\right|(\ell_2 s)\,j_2,\Omega+1\right\rangle$$

$$\left\langle(\ell_2 s)\,j_2,\Omega+2\left|r^\lambda Y_{\lambda 2}\right|(\ell_1 s)\,j_1,\Omega\right\rangle$$

$$= \;\delta\left((-1)^{\ell_1+\ell_2},(-1)^\lambda\right)\left\langle\ell_2 j_2\left|r^\lambda\right|\ell_1 j_1\right\rangle(-1)^{j_1+j_2+1+\lambda}(-1)^{\Omega-1/2}\sqrt{\frac{(2j_1+1)(2j_2+1)}{4\pi(2\lambda+1)}}$$

$$C(j_2 j_1\lambda;1/2,-1/2,0)\;\;C(j_2 j_1\lambda;\Omega+2,-\Omega,2)$$

$$= \;\left\langle(\ell_1 s)\,j_1,\Omega\left|r^\lambda Y_{\lambda-2}\right|(\ell_2 s)\,j_2,\Omega+2\right\rangle$$

Table 3 (continued)

($s_{\pm} = s_x \pm i\, s_y$ etc.)

$$\langle \ell_2 j_2 | \ell_1 j_1 \rangle \equiv \int_0^\infty dr R_{\ell_2 j_2}(r) R_{\ell_1 j_1}(r)$$

$$\langle (\ell_2 s) j_2, \Omega+1 | s_+ | (\ell_1 s) j_1, \Omega \rangle$$

$$= \delta(\ell_1, \ell_2)(-1)^{\ell_1 + j_1 + 1/2} \sqrt{3(2 j_1 + 1)} \; C(j_{1,} 1, j_2; \Omega, 1, \Omega+1) \; W(1/2, j_2, 1/2, j_1; \ell_1 1) \langle \ell_2 j_2 | \ell_1 j_1 \rangle$$

$$\langle (\ell_2 s) j_2, \Omega+1 | \ell_+ | (\ell_1 s) j_1, \Omega \rangle$$

$$= \delta(\ell_1, \ell_2)(-1)^{\ell_1 + j_2 - 1/2} \sqrt{2(2 j_1 + 1)} \sqrt{\ell_1(\ell_1 + 1)(2\ell_1 + 1)} \; C(j_1 1 j_2; \Omega, 1, \Omega+1) \; W(\ell_2 j_2 \ell_1 j_1; 1/2, 1)$$

$$\langle \ell_2 j_2 | \ell_1 j_1 \rangle$$

$$\langle (\ell_2 s) j_2, \Omega+1 | j_+ | (\ell_1 s) j_1, \Omega \rangle = \delta(j_1, j_2) \sqrt{(j - \Omega)(j + \Omega + 1)} \; \langle \ell_2 j_2 | \ell_1 j_1 \rangle$$

$$\langle (\ell_2 s) j_2, \Omega | s_z | (\ell_1 s) j_1, \Omega \rangle$$

$$= \delta(\ell_1, \ell_2)(-1)^{\ell_1 + j_1 - 1/2} \sqrt{\frac{3(2 j_1 + 1)}{2}} \; C(j_1, 1, j_2; \Omega, 0, \Omega) \; W(1/2, j_2, 1/2, j_1; \ell_1 1) \; \langle \ell_2 j_2 | \ell_1 j_1 \rangle$$

$$\langle (\ell_2 s) j_2, \Omega | \ell_z | (\ell_1 s) j_1, \Omega \rangle$$

$$= \delta(\ell_1, \ell_2)(-1)^{\ell_1 + j_2 + 1/2} \sqrt{2 j_1 + 1} \sqrt{\ell_1(\ell_1 + 1)(2\ell_1 + 1)} \; C(j_1 1 j_2; \Omega 0 \Omega) \; W(\ell_2 j_2 \ell_1 j_1; 1/2, 1)$$

$$\langle \ell_2 j_2 | \ell_1 j_1 \rangle$$

Table 3 (continued)

Phase convention in wave functions - important in non-diagonal matrix-elements

1) The coupling order of spin and orbit angular momentum ;

(ℓs)j or (sℓ)j ; $\left|(s\ell)j\right\rangle = (-1)^{\frac{1}{2}+\ell-j}\left|(\ell s)j\right\rangle$

2) Angular part of one-particle wave functions is defined by ;

$Y_{\ell m_\ell}(\theta,\phi)$ or $i^\ell Y_{\ell m_\ell}(\theta,\phi)$

3) The phase convention of $R_{\ell j}(r)$;

$$R_{\ell j}(r) \begin{cases} > 0 \ \ (\text{or} \ < 0) \quad \text{for } r \to 0 , \quad \text{or} \\ > 0 \ \ (\text{or} \ < 0) \quad \text{for } r \to \text{very large}, \quad \text{or} \\ \text{output of computers} \end{cases}$$

5. Weakly-bound and resonant neutron levels in Y_{20} deformed potential

~~harmonic-oscillator potential~~

[N n_z Λ Ω]

5.1. Weakly-bound neutrons

Remember the Nilsson diagram based on
modified oscillator Hamiltonian
for the *sd*-shell →

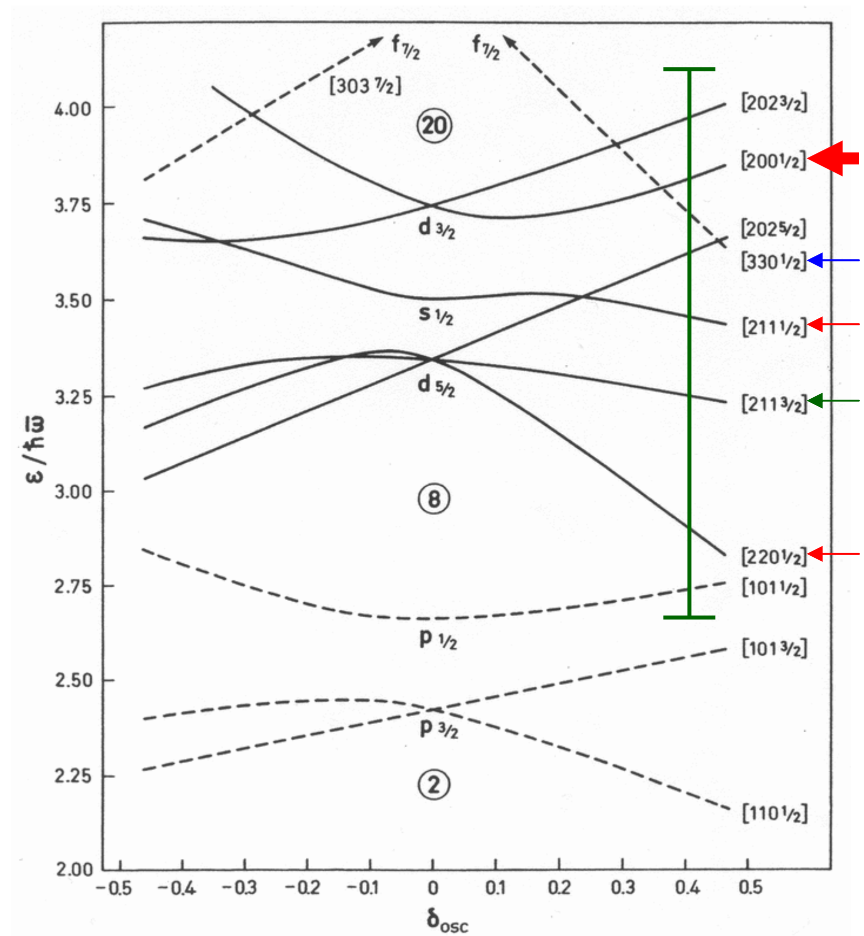

A.Bohr and B.R.Mottelson, vol.2, Figure 5-1.

6 doubly-degenerate levels in *sd*-shell

3 $\Omega^{\pi}=1/2^{+}$ ($\ell_{min}=0$)
2 $\Omega^{\pi}=3/2^{+}$ ($\ell_{min}=2$)
1 $\Omega^{\pi}=5/2^{+}$ ($\ell_{min}=2$)

} 12 particles

As ε_Ω (<0) → 0, the structure of one-particle wave-functions may deviate from $[N\ n_z\ \Lambda\ \Omega]$, even for $|\beta|$ → large.
Nevertheless, one-particle levels are denoted by original $[N\ n_z\ \Lambda\ \Omega]$.

$\Omega^\pi = 1/2^+$ one-particle level has $\ell_{min} = 0$ component.

ex. Radial wave functions of the [200 ½] level in Woods-Saxon potentials.

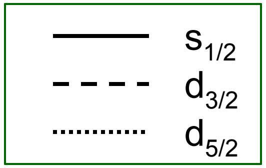

(The radius of potentials is adjusted to obtain respective eigenvalues ε_Ω .)

Bound state with ε_Ω = -8.0 MeV.

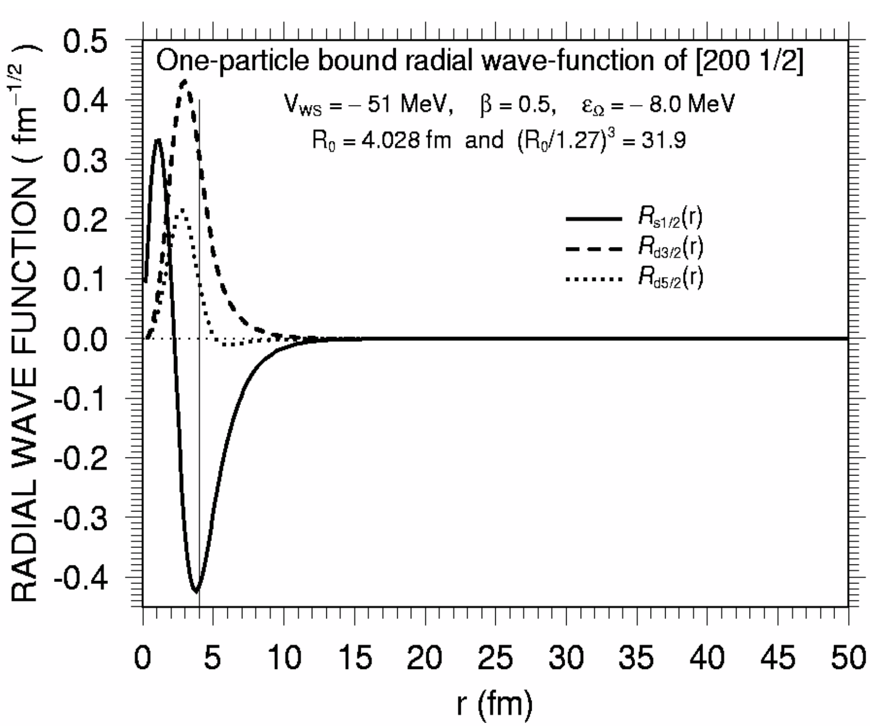

Similar behavior to wave functions in harmonic osc. potentials.

Bound state with ε_Ω = -0.0001 MeV.

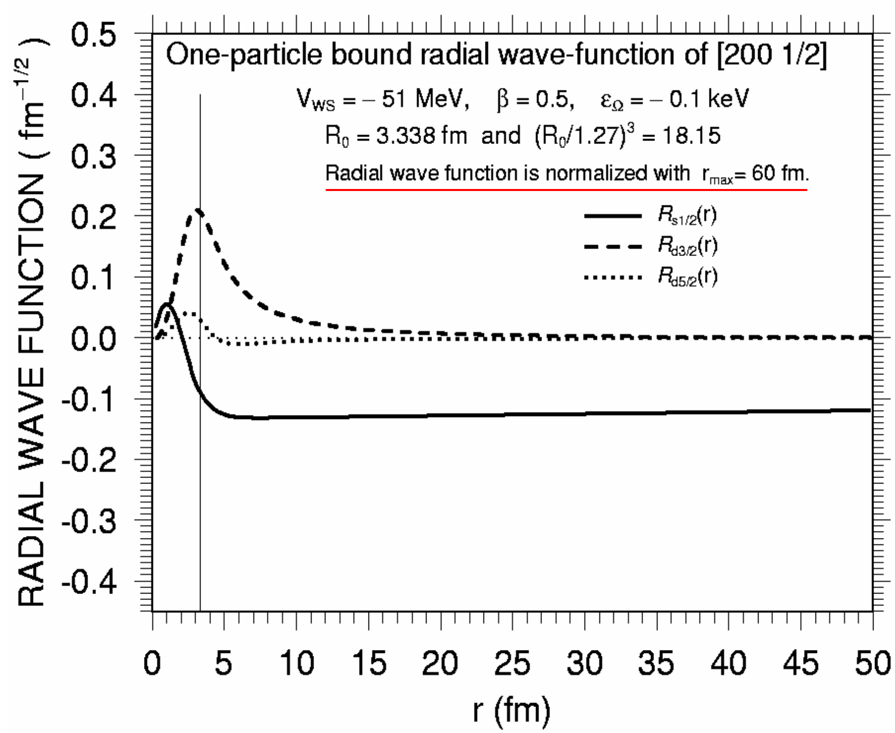

Wave functions unique in finite-well potentials.

For $\varepsilon \to 0$, the *s*-dominance will appear in all $\Omega^\pi = 1/2^+$ bound orbits. However, the energy, at which the dominance shows up, depends on both deformation and respective orbits.

ex. Calculated $s_{1/2}$ probability in three $\Omega^\pi = 1/2^+$ Nilsson orbits in the *sd*-shell as a function of energy eigenvalue ε_Ω .

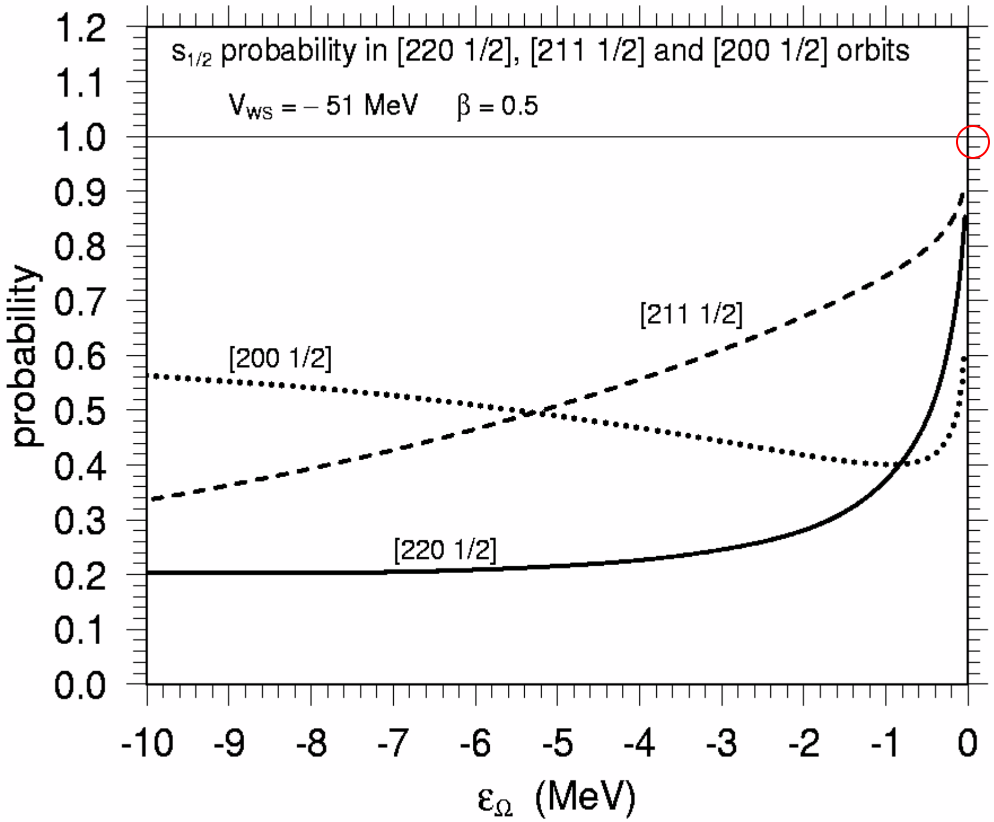

Deformed halo nuclei

$\ell_{min}=0$

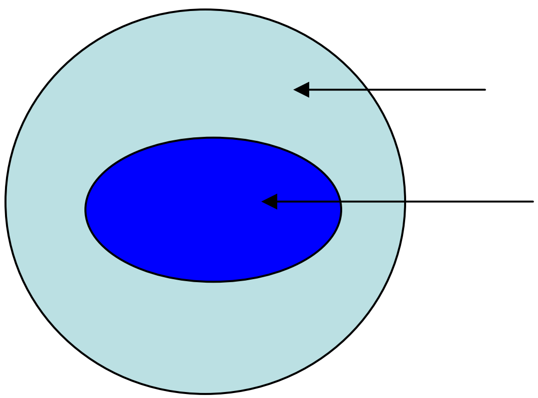

$\Omega^{\pi}=1/2^{+}$ neutron orbit $\rightarrow$ $s_{1/2}$, as $|\varepsilon_{\Omega}| \rightarrow 0$.

deformed core

, irrespective of the size of deformation and the kind of one-particle orbits.

The rotational spectra of deformed halo nuclei must come from the deformed core.

Ex. Ω^{π} = 1/2 $^{-}$ and 3/2 $^{-}$ one-particle levels have $\ell_{min} = 1$ component.

The *p*-components increase as $\varepsilon_{\Omega} \to 0$, but the probability at $\varepsilon_{\Omega} = 0$ depends on respective levels, deformations, and the diffuseness of potentials.

Calculated probabilities of (ℓ j) components of one-particle [N n_z Λ Ω] levels in the *pf* shell as a function of energy eigenvalue ε_{Ω} .

[330 1/2] orbit

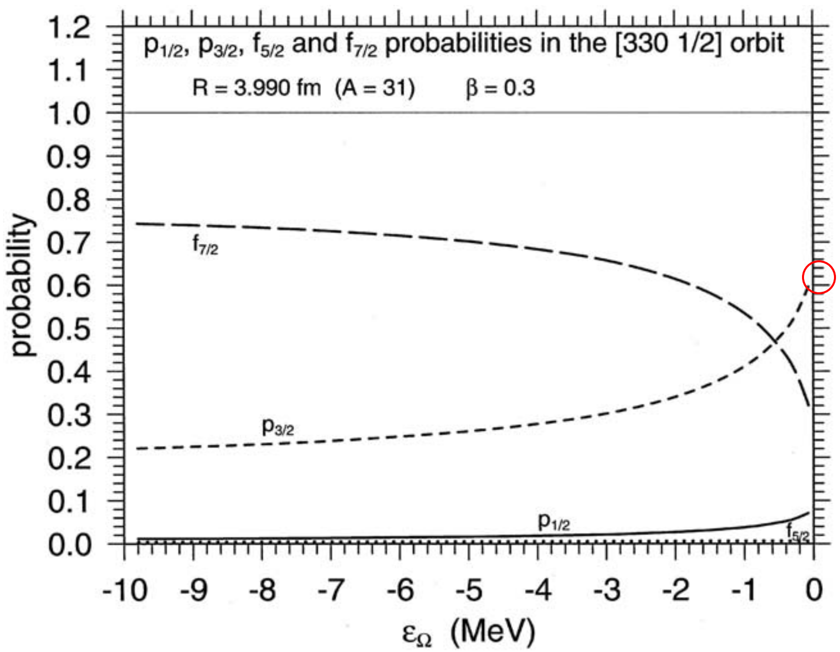

[321 3/2] orbit

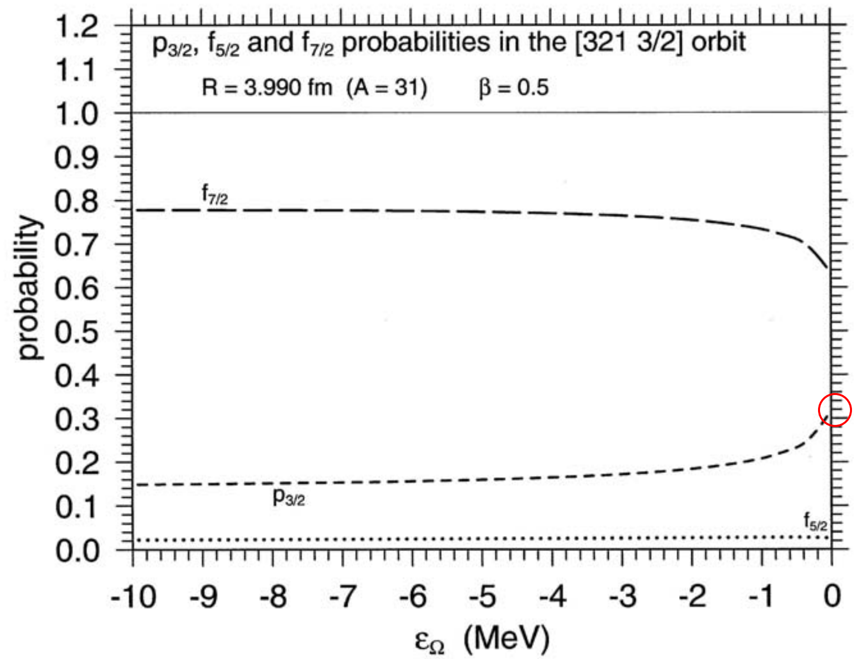

5.2. One-particle resonant levels in deformed potential – eigenphase formalism

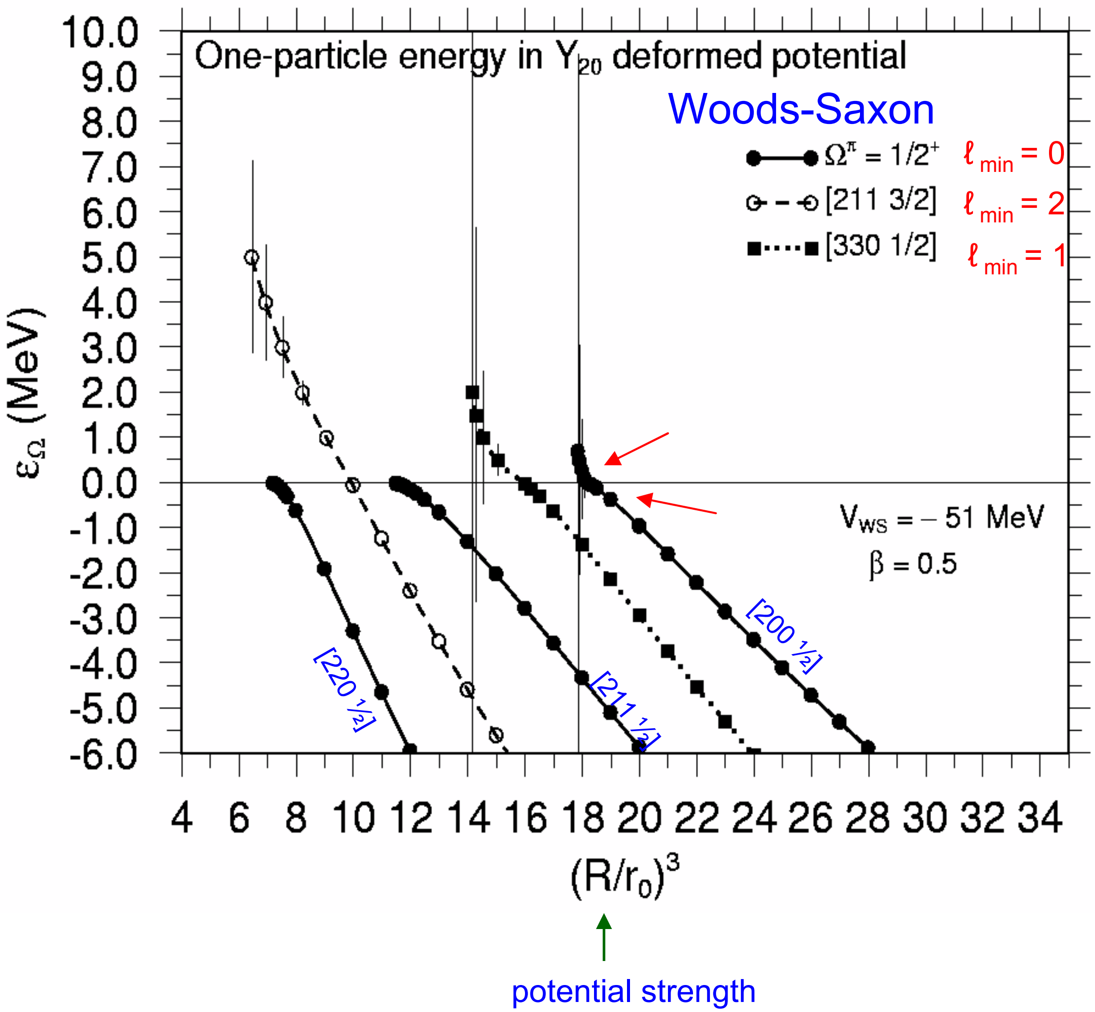

1) The majority of bound ($\varepsilon_{\Omega} < 0$) neutron $\Omega^{\pi} = 1/2^{+}$ levels do not continue to one-particle resonant levels for $\varepsilon_{\Omega} > 0$.
Even the resonant levels surviving for very small $\varepsilon_{\Omega} > 0$ die out at small ε_{Ω}, if an appreciable amount of $\ell_{min} = 0$ component is contained in wave functions.

2) The ℓ_{min} value in the components of deformed wave functions is crucial for both the width of one-particle resonant levels and up till which value of ε_{Ω} (> 0) the resonant level can survive.

3) One-particle levels die out at smaller ε_{Ω} (>0) values, for the potential with a larger diffuseness.

W-S potential parameters are fixed except radius *R*.

($r_0 = 1.27$ fm is used.)

Radial wave functions of the [200 ½] level

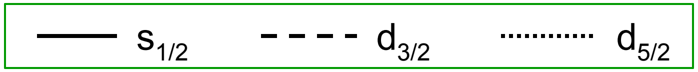

The potential radius is adjusted to obtain respective eigenvalue ($\varepsilon_\Omega < 0$) and resonance ($\varepsilon_\Omega > 0$).

Bound state with $\varepsilon_\Omega = -\ 0.1$ keV

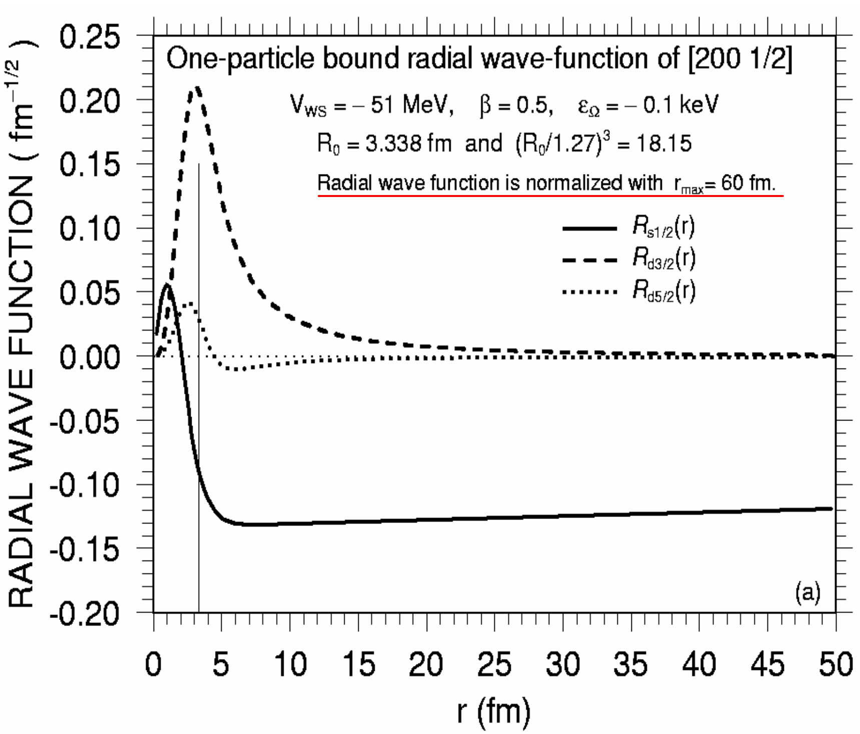

Resonant state with $\varepsilon_\Omega = +100$ keV

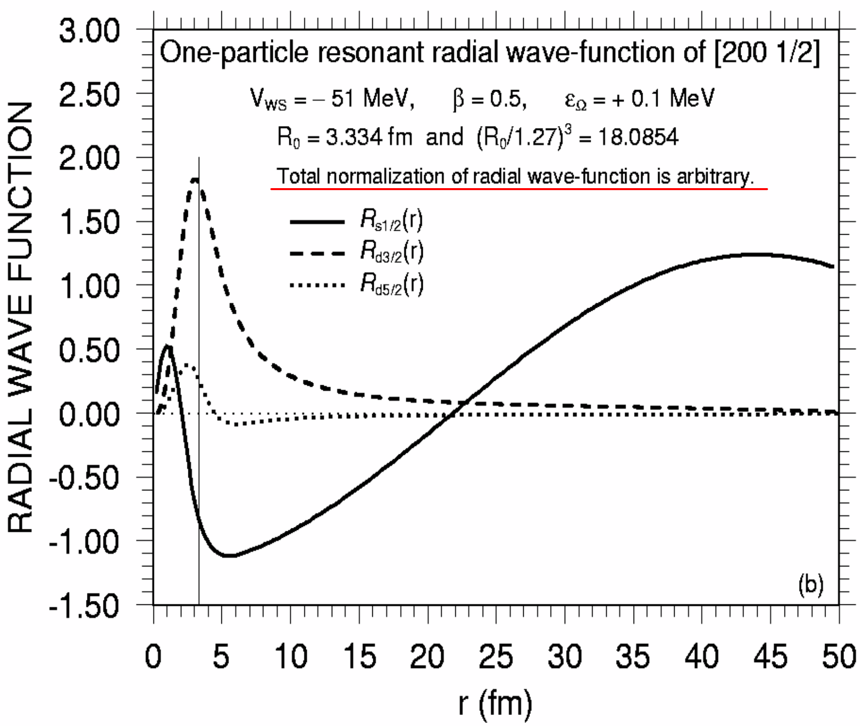

Existence of resonance ← d component
Width of resonance ← s component

OBS. Relative amplitudes of various components inside the potential remain nearly the same for $\varepsilon_\Omega = -\ 0.1$ keV ⟶ + 100 keV.

Neutron resonant levels in deformed potential

One-particle resonant levels in deformed potentials are defined using eigenphase formalism :

One eigenphase δ_Ω increases through $\pi/2$ as ε_Ω increases

$\longrightarrow$ one-particle resonance in deformed potential

I.H., Phys.Rev. C**72**, 024301 (2005); C**73**, 064308 (2006)

R.G.Newton, Scattering Theory of Waves and Particles (McGraw-Hill, New York, 1966)

(Among an infinite number of positive-energy one-particle levels, one-particle resonant levels are most important in the construction of many-body correlations of nuclear bound states.)

In the limit of $\beta \to 0$ the definition of one-particle resonance in the eigenphase formalism

$\longrightarrow$ the definition in spherical potentials in terms of phase shift.

Do not restrict the system in a finite box !

For $\varepsilon_\Omega < 0$

$$R_{\ell j\Omega}(r) \propto r k_\ell(\alpha_b r) \qquad \text{for} \qquad r \to \infty$$

where $k_\ell(\alpha_b r)$ is the modified spherical Bessel function of the third kind, and

$$\alpha_b^2 \equiv -\frac{2m\varepsilon_\Omega}{\hbar^2}$$

For $\varepsilon_\Omega > 0$

$$R_{\ell j\Omega}(r) \propto \cos(\delta_\Omega) r j_\ell(\alpha_c r) - \sin(\delta_\Omega) r n_\ell(\alpha_c r) \qquad \text{for} \qquad r \to \infty$$

$$\to \sin(\alpha_c r + \delta_\Omega - \ell\frac{\pi}{2})$$

where $$\alpha_c^2 \equiv \frac{2m}{\hbar^2}\varepsilon_\Omega$$

δ_Ω : eigenphase common to all ℓj channels

Due to the axially-symmetric deformation, radial wave-functions $R_{\ell j\Omega}(r)$ for a given Ω but different ℓj values are coupled. All (ℓj) components of a solution of coupled-channel equations have a common eigenphase.

A given eigenchannel : asymptotic radial wave-functions behave in the same way for all (ℓj) components.

One-particle resonant level in a deformed potential :

one of eigenphases δ_Ω increases through $\pi/2$ as ε_Ω increases.

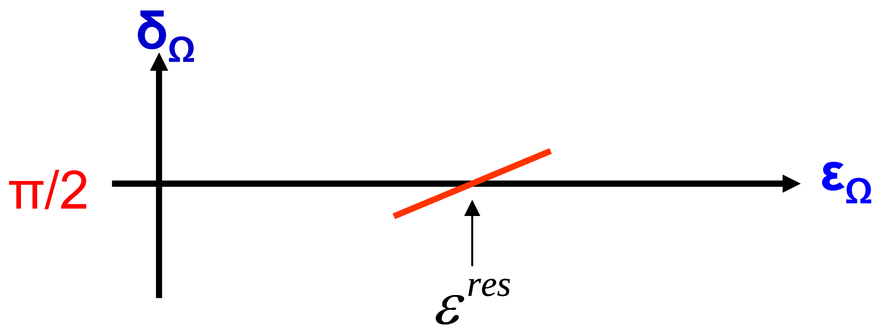

When one-particle resonant level in terms of one eigenphase is obtained, the width Γ_Ω of the resonance in the intrinsic system is calculated by

$$\Gamma_\Omega \equiv \frac{2}{\left[\dfrac{d\delta_\Omega}{d\varepsilon_\Omega}\right]_{\varepsilon_\Omega=\varepsilon_\Omega^{res}}}$$

: intrinsic width

I.H., Phys. Rev. C73, 064308 (2006)

Some comments on eigenphase ;

1) For a given potential and a given ε_Ω
there are several (in principle, an infinite number of) solutions of eigenphase δ_Ω .

2) The number of eigenphases for a given potential and a given ε_Ω is equal to that of wave function components with different (ℓ,j) values.

3) The value of δ_Ω determines the relative amplitudes of different (ℓ,j) components.

4) In the region of small values of ε_Ω (> 0), only one of eigenphases varies strongly as a function of ε_Ω , while other eigenphases remain close to the values of $n\pi$.

I.H., PRC **76** (2007) 054319;
I.H., J. Phys. G, **37** (2010) 055102

5.3. Examples of Nilsson diagrams for lighter neutron-rich nuclei

1. ~ $^{17}C_{11}$ (S(n) = 0.73 MeV, $3/2^+$)
2. ~ $^{31}Mg_{19}$ (S(n) = 2.38 MeV, $1/2^+$)
   ~ $^{33}Mg_{21}$ (S(n) = 2.22 MeV, $3/2^-$)
3. ~ $^{31}Ne_{21}$ (S(n) = 0.29 ± 1.64 MeV, halo structure)
4. ~ $^{37}Mg_{25}$ (S(n) = a few hundreds keV ?)
5. ~ $^{41}Si_{27}$ (S(n) = 1.34 ± 0.57 MeV)
6. ~ $^{45}S_{29}$ (S(n) = 2.86 ± 0.77 MeV)
7. A ~ 75 region

Near degeneracy of some weakly-bound or resonant levels in spherical potential, unexpected from the knowledge on stable nuclei

- the origin of deformation and …….

Jahn-Teller effect

One-particle neutron energies as a function of quadrupole deformation β

N ~ 8 region

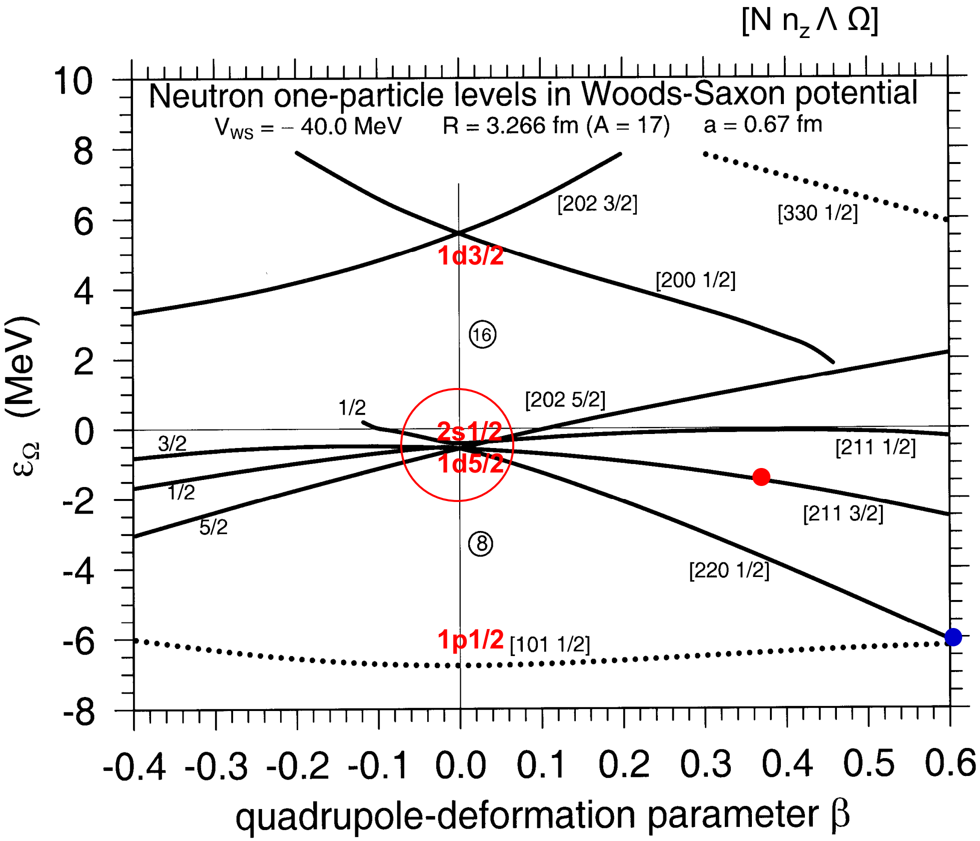

At $\beta=0$;
$\varepsilon(2s_{1/2})-\varepsilon(1d_{5/2})$
= 140 keV

● $^{17}C_{11}$ (3/2+) S(n) = 0.73 MeV

● $^{11}Be_7$ ($1/2^+$) S(n) = 0.50 MeV

½ -	——	0.32
½ +	——	0

β ~ 0.7

in ^{12}Be from (p,p')

In μ_{calc} $\left\{ \begin{array}{l} g_R = 0.35 \quad \text{(for } \beta\neq 0\text{)} \\ g_s^{eff} = g_s^{free} \end{array} \right\}$ are used.

Nucleus	S(n) (keV)	I^π	μ_{obs} (μ_N)	Reference	μ_{calc} (at β, [N n_z Λ Ω]) (μ_N)
$^{17}C_{11}$	727	$3/2^+$	$\pm 0.758(4)$	[12]	-0.75 (β=0.4, [211 3/2])
$^{11}Be_7$	504	$1/2^+$	$-1.6816(8)$	[13]	-1.7 (β=0.6, [220 1/2])
$^{15}C_9$	1218	$1/2^+$	$\pm 1.720(9)$	[11]	-1.9 (β=0, $2s_{1/2}$)

[12] H.Ogawa et al., Eur.Phys.J. **A 13** (2002) 81
H.Ueno et al., N.P.**A738** (2004) 211

[13] W.Geithner et al., PRL **83** (1999) 3792

[11] K.Asahi et al., N.P.**A704** (2002) 88c

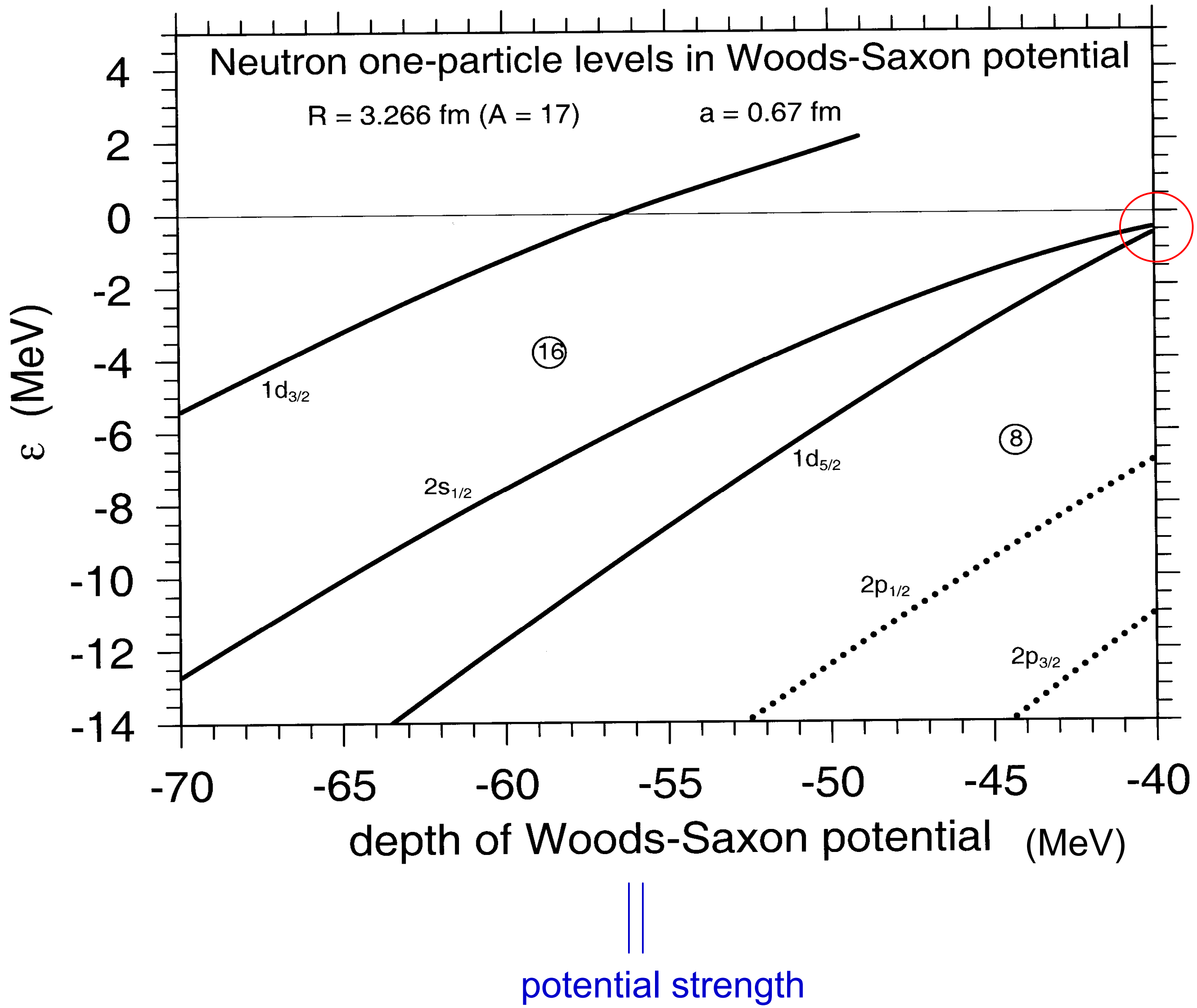
Neutron one-particle levels in Woods-Saxon potential
R = 3.266 fm (A = 17)
a = 0.67 fm
1d3/2
2s1/2
1d5/2
2p1/2
2p3/2
16
8
4
2
0
-2
-4
-6
-8
-10
-12
-14
ε (MeV)
-70
-65
-60
-55
-50
-45
-40
depth of Woods-Saxon potential (MeV)
||
potential strength

One-particle neutron energies as a function of quadrupole deformation β

N ~ 20 region

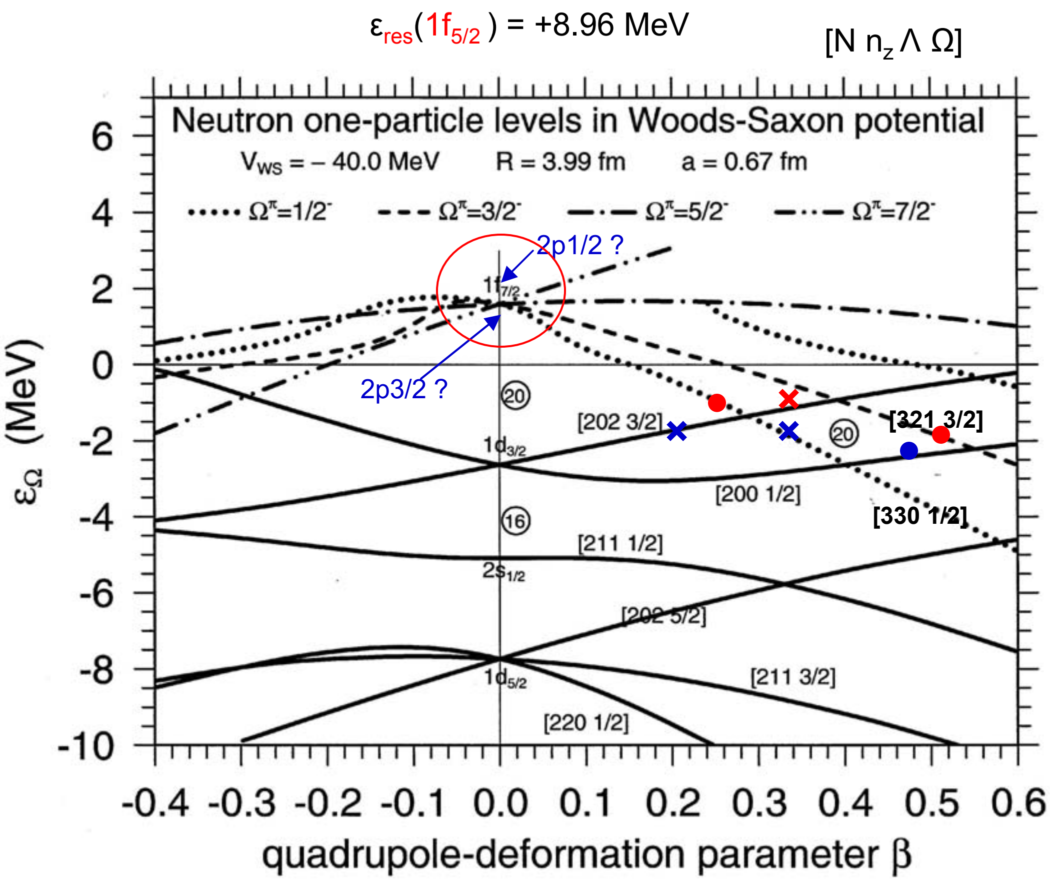

Resonant states at $\beta=0$;
$\varepsilon_{res}(2p_{3/2}) < \varepsilon_{res}(1f_{7/2})$

● $^{33}Mg_{21}$ S(n) = 2.22 MeV

● $^{31}Mg_{19}$ S(n) = 2.38 MeV

× or × are excluded by the sign of measued magnetic moments.

In μ_{calc} $\left\{ \begin{array}{l} g_R = 0.38 \quad \text{(for } \beta\neq 0) \\ g_s^{eff} = (0.7) g_s^{free} \end{array} \right\}$ are used.

Then, $\mu_{calc}(f_{7/2}) = -1.3\mu_N$

$\mu_{calc}(d_{3/2}) = +0.80\mu_N$

Nucleus	S(n) (keV)	$(I^\pi)_{obs}$	μ_{obs} (μ_N)	Reference	$(I^\pi)_{cal}$	μ_{calc} (at β, [N nz Λ Ω]) (μ_N)
$^{33}Mg_{21}$	2222	3/2	−0.7456(5)	[16]	$3/2^-$	−0.88 (β=0.25, [330 1/2])
					$3/2^+$	+0.91 (β=0.35, [202 3/2])
					$3/2^-$	−0.39 (β=0.45, [321 3/2])
$^{31}Mg_{19}$	2378	$1/2^+$	−0.88355(15)	[14]	$1/2^+$	−1.00 (β=0.45, [200 1/2])
					$3/2^-$	−0.91 (β=0.35, [330 1/2])

[16] D.T.Yordanov et al., PRL **99** (2007) 212501

[14] G.Neyens et al., PRL **94** (2005) 022501

I.H., J. Phys. G, **37** (2010) 055102

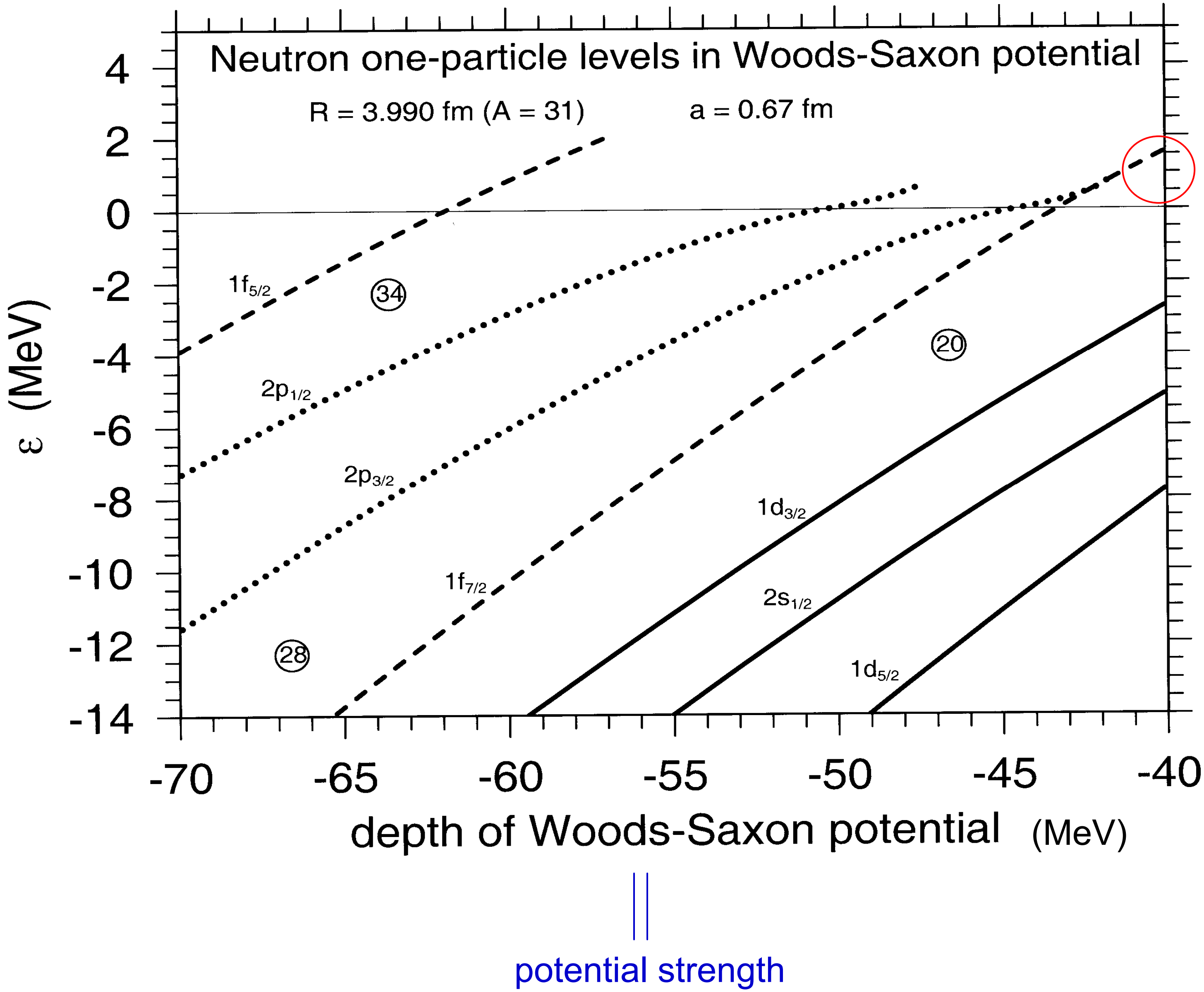
Neutron one-particle levels in Woods-Saxon potential
R = 3.990 fm (A = 31)
a = 0.67 fm
ε (MeV)
4
2
0
-2
-4
-6
-8
-10
-12
-14
1f5/2
2p1/2
2p3/2
1f7/2
1d3/2
2s1/2
1d5/2
34
20
28
-70
-65
-60
-55
-50
-45
-40
depth of Woods-Saxon potential (MeV)
||
potential strength

One-particle neutron energies as a function of quadrupole deformation β

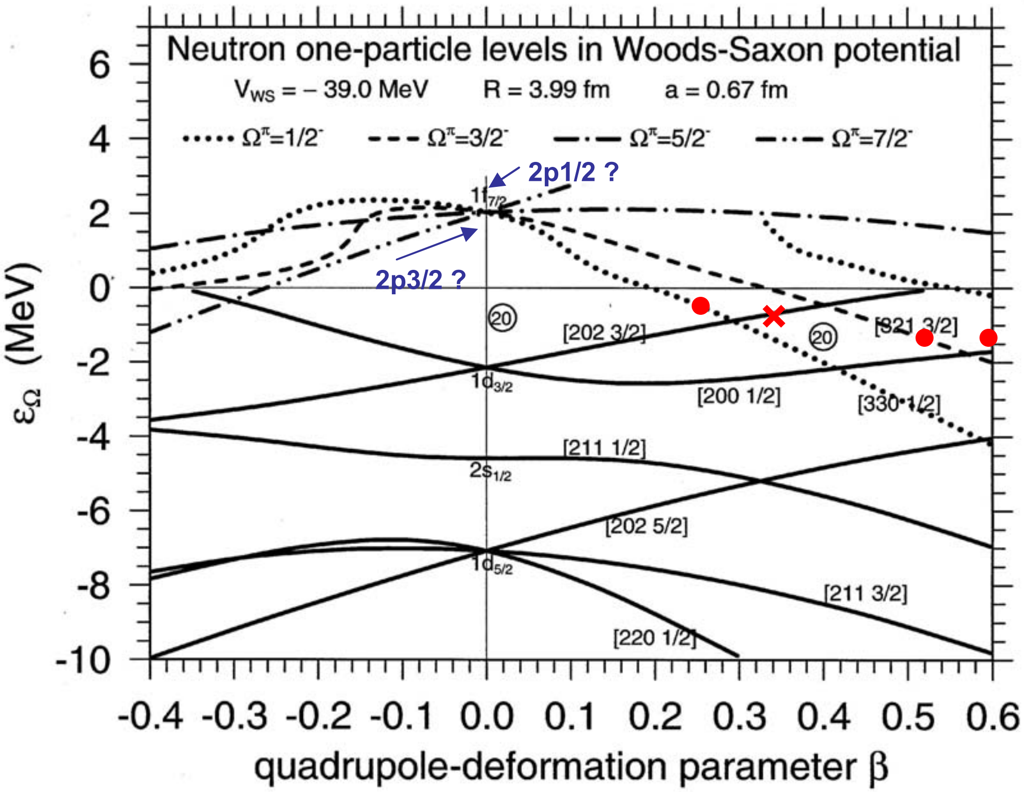

$[N\ n_z\ \Lambda\ \Omega]$

● $^{31}Ne_{21}$ S(n) = 0.29 ± 1.64 MeV

T.Nakamura, N.Kobayashi, Y.Kondo, Y.Satou, et al., PRL **103**, 262501 (2009), Coulomb breakup of 31Ne → halo structure

The 21st neutron cannot be placed on × in [202 3/2] because of observed halo structure.

$I^\pi =$

$3/2^-$	from	[330 1/2]	for	$0.20 < \beta < 0.30$	←	$p(\ell = 1)$ halo
$3/2^+$	from	[202 3/2]	for	$0.30 < \beta < 0.40$	←	no halo $(\because\ \ell_{\min} = 2)$
$3/2^-$	from	[321 3/ 2]	for	$0.40 < \beta < 0.58$	←	$p(\ell = 1)$ halo
$1/2^+$	from	[200 1/2]	for	$\beta > 0.58$	←	$s(\ell = 0)$ halo

One-particle neutron energies as a function of quadrupole deformation β

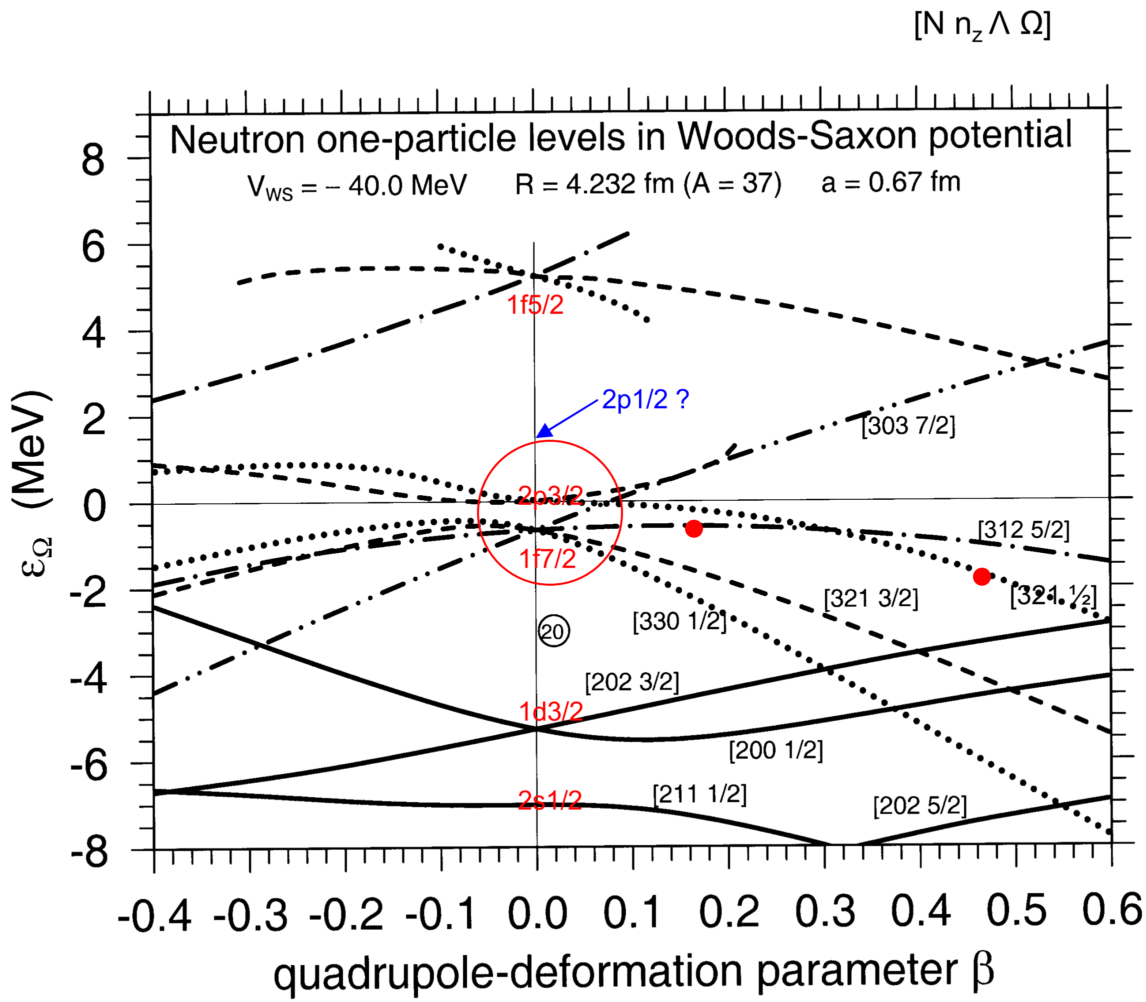

In the case of very weak binding
N=28 is not a magic number !

At β=0 ;
$\varepsilon(2p_{3/2}) - \varepsilon(1f_{7/2})$
= 680 keV

● $^{37}Mg_{25}$ S(n) = a few hundreds keV ?

$$I^{\pi} = \begin{cases} 5/2^{-} \text{ from } [312\ 5/2] \text{ for } 0 < \beta < 0.3 & \leftarrow \text{no halo } (\because\ \ell_{min} = 3) \\ 1/2^{-} \text{ from } [321\ 1/2] \text{ for } 0.3 < \beta < 0.6 & \leftarrow p(\ell = 1) \text{ halo} \end{cases}$$

One-particle neutron energies as a function of quadrupole deformation β

N ~ 28 region

[N n_z Λ Ω]

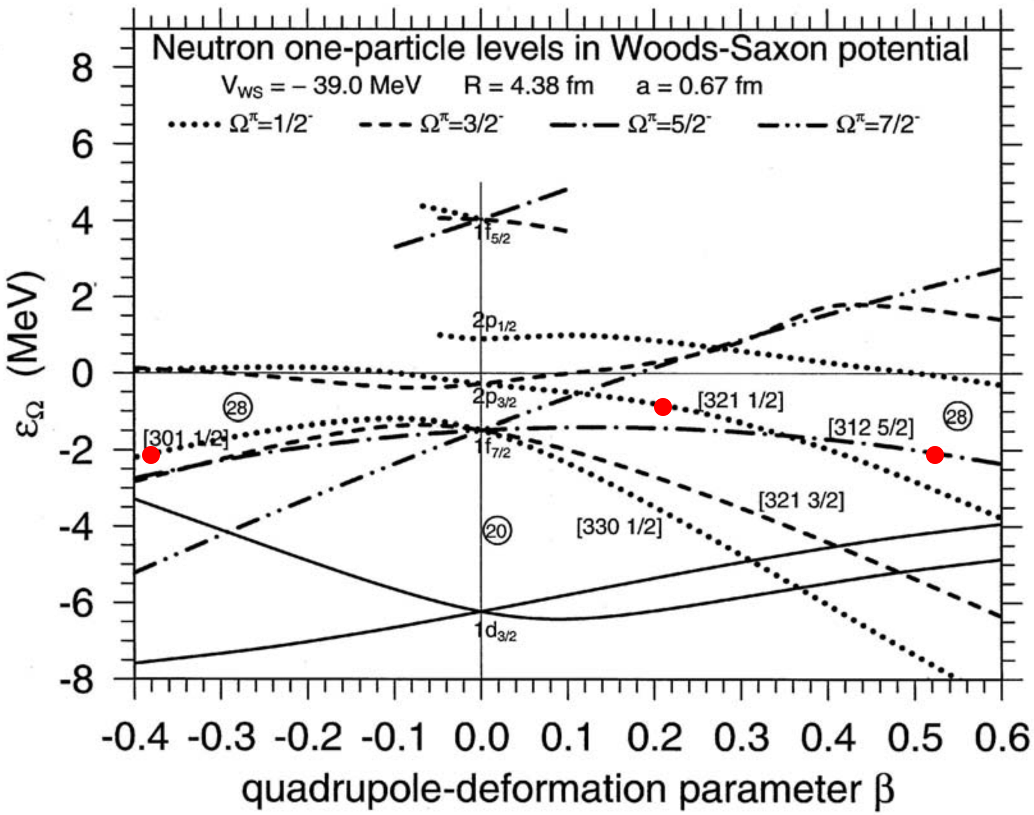

At $\beta=0$;

$\varepsilon(2p_{3/2}) - \varepsilon(1f_{7/2}) = 1.20$ MeV

● $^{41}Si_{27}$ S(n) = 1.34 ± 0.6 MeV

In μ_{calc} $\left\{ \begin{array}{l} g_R = 0.38 \quad \text{(for } \beta\neq0) \\ g_s^{eff} = (0.7) g_s^{free} \end{array} \right\}$ are used.

Then,

$$\mu_{calc}(p_{1/2}) = +0.4\mu_N$$
$$\mu_{calc}(p_{3/2}) = -1.3\mu_N$$
$$\mu_{calc}(f_{7/2}) = -1.3\mu_N$$

Nucleus	S(n) (MeV)	$(I^\pi)_{cal}$	μ_{calc} (at β, [N n_z Λ Ω]) (μ_N)
$^{41}Si_{27}$	1.34	$3/2^-$	+0.07 (β=−0.4, [301 1/2])
		$3/2^-$	−0.66 (β=0.25, [321 1/2])
		$5/2^-$	−0.58 (β=0.45, [312 5/2])

Cf. In $^{43}S_{27}$ the 320 keV isomeric state has $7/2^-$ from g-factor measurement → The ground state is deformed ?

One-particle neutron energies as a function of quadrupole deformation β

N ~ 28 region

[N n_z Λ Ω]

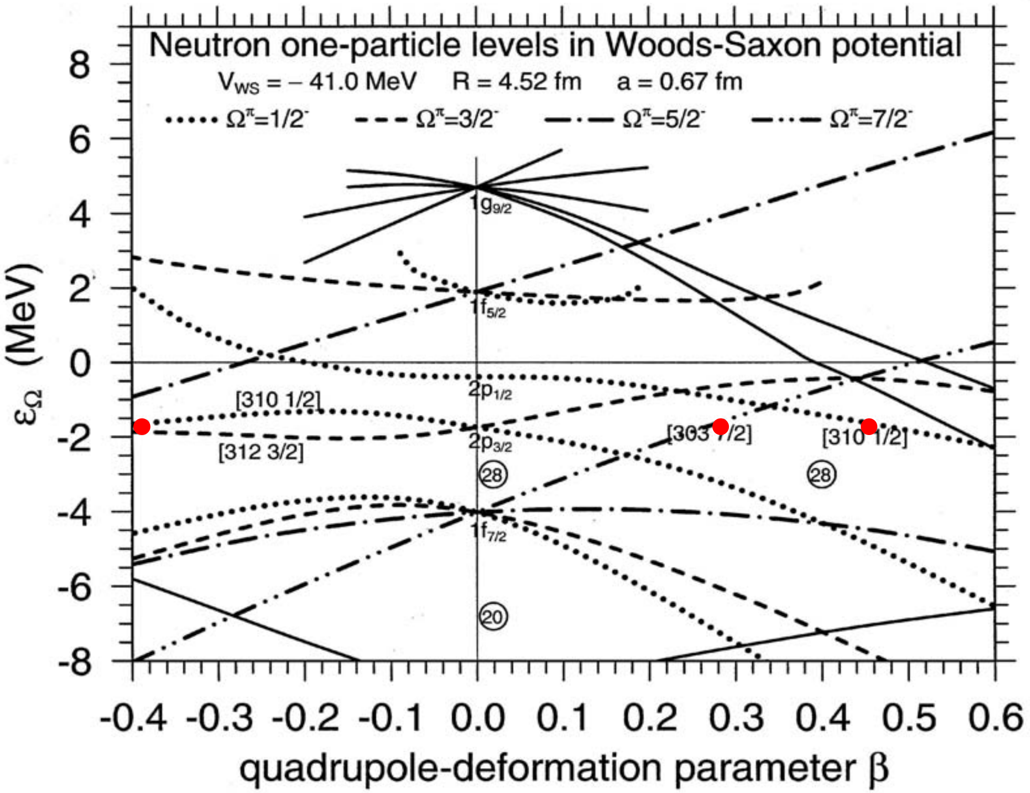

Nucleus	S(n) (MeV)	$(I^\pi)_{cal}$	μ_{calc} (at β, [N n_z Λ Ω]) (μ_N)
$^{45}S_{29}$	2.21	$7/2^-$	−0.74 ($\beta = 0.25$, [303 7/2])
		$1/2^-$	+0.59 (β=0.45, [310 1/2])
		$1/2^-$	+0.59 (β=−0.40, [310 1/2])
		$3/2^-$	+0.16 (β=−0.40, [312 3/2])

● $^{45}S_{29}$ S(n) = 2.86 ± 0.7 MeV

In μ_{calc} $\left\{ \begin{array}{l} g_R = 0.38 \ \text{(for β≠0)} \\ g_s^{eff} = (0.7) g_s^{free} \end{array} \right\}$ are used.

Then,

$$\mu_{calc}(p_{1/2}) = +0.4\mu_N$$

$$\mu_{calc}(p_{3/2}) = -1.3\mu_N$$

$$\mu_{calc}(f_{7/2}) = -1.3\mu_N$$

One-particle neutron energies as a function of quadrupole deformation β

N ~ 50 region

A ~ 75 region

$\varepsilon_{res}(1h_{11/2}) = +5.48$ MeV
$\varepsilon_{res}(1g_{7/2}) = +3.44$ MeV
at β=0

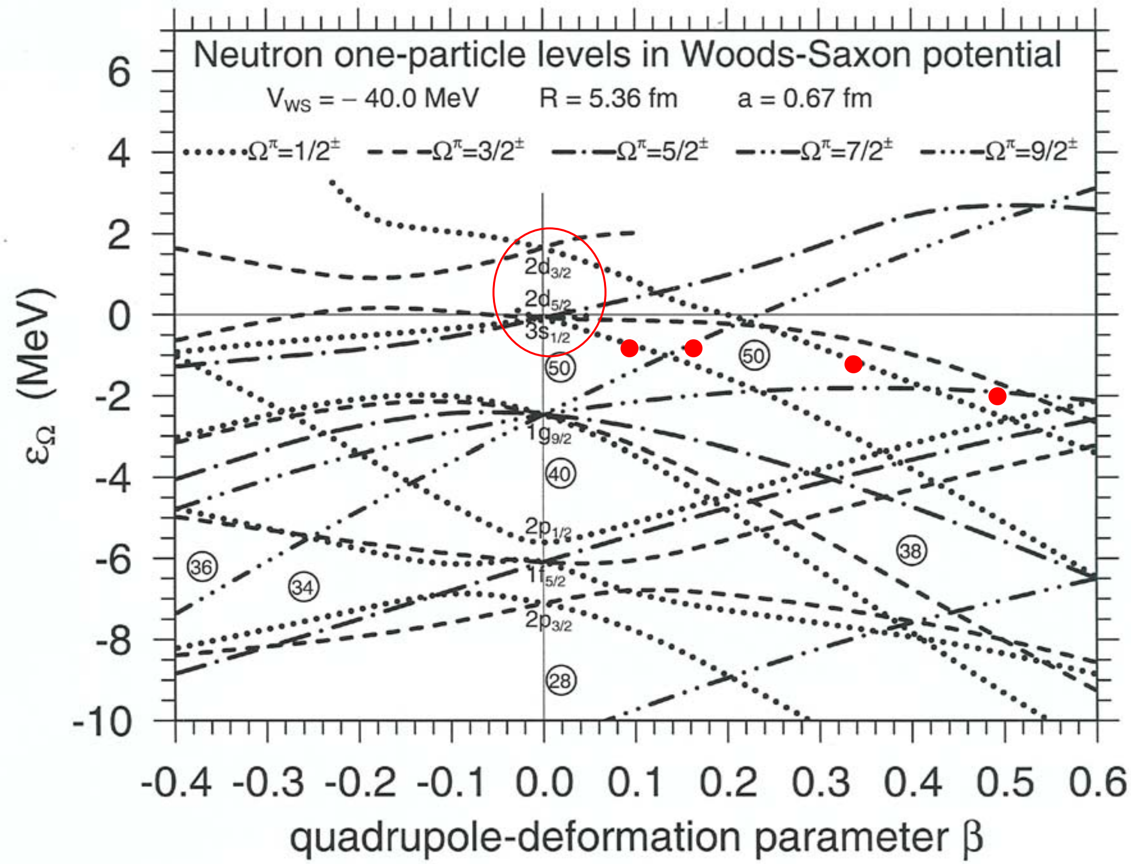

In the case of very weak binding

At β=0 ;
$\varepsilon(3s_{1/2}) < \varepsilon(2d_{5/2})$

● 51^{st} neutron

ex. ${}^{75}_{24}Cr_{51}$?

Neutron-drip-line nuclei with N=51have a good chance to have the ground or very low-lying $I^\pi = 1/2^+$ state, irrespective of spherical or deformed shape.

In lecture V.3 a way of calculating observed quantities in lab system using deformed intrinsic wave functions is shown, which can be of practical use though it involves an approximation. The set of basis wave functions given in V.3 are useful also for including rotational perturbation. Here, we show ;

Appendix. Angular momentum projection from a deformed intrinsic state $|\phi\rangle$

(not applicable when rotational perturbation of intrinsic states has to be included.)

Rotational operator $R(\Omega)$ $\quad\quad$ Ω : Euler angles (α, β, γ)

$$R(\Omega) \equiv e^{-i\alpha J_z} e^{-i\beta J_y} e^{-i\gamma J_z}$$

Rotation matrix $D^J_{MM'}(\Omega)$

$$\langle \alpha JM | R(\Omega) | \alpha' J' M' \rangle = \delta(\alpha, \alpha') \delta(J, J') D^J_{MM'}(\Omega)$$

Inverting the expression

$$R(\Omega) = \sum_{\alpha J} | \alpha JM \rangle D^J_{MM'}(\Omega) \langle \alpha JM' |$$

Multiplying by $D^{J\ *}_{MM'}(\Omega)$ and integrating over Ω, we obtain a projection operator

$$P^J_M \equiv \sum_{\alpha} | \alpha JM \rangle \langle \alpha JM | = \frac{2J+1}{8\pi^2} \int d\Omega D^{J\ *}_{MM}(\Omega) R(\Omega)$$

We need to calculate the expressions

$$\boxed{\begin{aligned} \langle \phi | P^J_M | \phi \rangle &= \frac{2J+1}{8\pi^2} \int d\Omega D^{J\ *}_{MM}(\Omega) \langle \phi | R(\Omega) | \phi \rangle \\ \langle \phi | H P^J_M | \phi \rangle &= \frac{2J+1}{8\pi^2} \int d\Omega D^{J\ *}_{MM}(\Omega) \langle \phi | H R(\Omega) | \phi \rangle \end{aligned}}$$

Appendix (continued)

If $|\phi\rangle$ is axially symmetric, $J_z|\phi\rangle = M|\phi\rangle$

$$\langle\phi|R(\Omega)|\phi\rangle = e^{-i\alpha M}\langle\phi|e^{-i\beta J_y}|\phi\rangle e^{-i\gamma M}$$

$$D^J_{MM}(\Omega) = e^{-i\alpha M}\langle JM|e^{-i\beta J_y}|JM\rangle e^{-i\gamma M}$$

then, using the "reduced rotation matrix" $d^J_{MM'}(\theta) = \langle JM|e^{-i\theta J_y}|JM'\rangle$

which describes the collective rotational motion, one obtains

$$\boxed{\begin{aligned}\langle\phi|P^J_M|\phi\rangle &= \frac{2J+1}{2}\int_0^\pi d\theta\sin\theta\, d^J_{MM}(\theta)\langle\phi|e^{-i\theta J_y}|\phi\rangle \\ \langle\phi|HP^J_M|\phi\rangle &= \frac{2J+1}{2}\int_0^\pi d\theta\sin\theta\, d^J_{MM}(\theta)\langle\phi|He^{-i\theta J_y}|\phi\rangle\end{aligned}}$$

where the overlap functions :

$$\langle\phi|e^{-i\theta J_y}|\phi\rangle \begin{cases} \approx 1 \quad \text{for} \quad \theta << 1\text{ ,} \\ \text{decreases quickly as } \theta \rightarrow \text{larger (at least in heavier deformed nuclei),} \\ \text{is symmetric about } \theta = \pi/2\text{ .}\end{cases}$$